Self-Healing Polymers and Composites

B.J. Blaiszik,[1,2] S.L.B. Kramer,[1,2] S.C. Olugebefola,[2]
J.S. Moore,[2,3] N.R. Sottos,[1,2] and S.R. White[2,4,*]

[1]Department of Materials Science and Engineering, [2]Beckman Institute for Advanced Science
and Technology, [3]Department of Chemistry, and [4]Department of Aerospace Engineering,
University of Illinois, Urbana-Champaign, Urbana, Illinois 61801; email: blaiszik@illinois.edu,
sbkramer@illinois.edu, solar@illinois.edu, jsmoore@illinois.edu, n-sottos@illinois.edu,
swhite@illinois.edu

*Corresponding author

Key Words

bioinspired, remendable, autonomic, capsule, vascular, intrinsic

Abstract

Self-healing polymers and fiber-reinforced polymer composites possess the
ability to heal in response to damage wherever and whenever it occurs in the
material. This phenomenal material behavior is inspired by biological sys-
tems in which self-healing is commonplace. To date, self-healing has been
demonstrated by three conceptual approaches: capsule-based healing sys-
tems, vascular healing systems, and intrinsic healing polymers. Self-healing
can be autonomic—automatic without human intervention—or may require
some external energy or pressure. All classes of polymers, from thermosets
to thermoplastics to elastomers, have potential for self-healing. The major-
ity of research to date has focused on the recovery of mechanical integrity
following quasi-static fracture. This article also reviews self-healing during
fatigue and in response to impact damage, puncture, and corrosion. The con-
cepts embodied by current self-healing polymers offer a new route toward
safer, longer-lasting, fault-tolerant products and components across a broad
cross section of industries including coatings, electronics, transportation,
and energy.

1. INTRODUCTION

Self-healing: the ability to repair damage and restore lost or degraded properties or performance using resources inherently available to the system

Autonomic healing: self-healing that occurs automatically without human intervention

Degradation, damage, and failure are natural consequences of material applications. Engineering research has been focused traditionally on either the design of new materials with increased robustness or the development of nondestructive evaluation methods for material inspection, yet all engineered materials eventually fail. In contrast, biological systems approach this same dilemma in an elegant fashion: by self-healing. Self-healing materials exhibit the ability to repair themselves and to recover functionality using the resources inherently available to them. Whether the repair process is autonomic or externally assisted (e.g., by heating), the recovery process is triggered by damage to the material. Self-healing materials offer a new route toward safer, longer-lasting products and components.

Biology provides an abundance of self-healing systems that embody the guiding principles behind the design of synthetic versions. In either case, the initial response is triggered by injury (**Figure 1**). Biological response is threefold: inflammatory response (immediate), cell proliferation (secondary), and matrix remodeling (long-term). Synthetic systems share this three-step process, albeit in a more simplistic fashion and at an accelerated rate. The first response is triggering
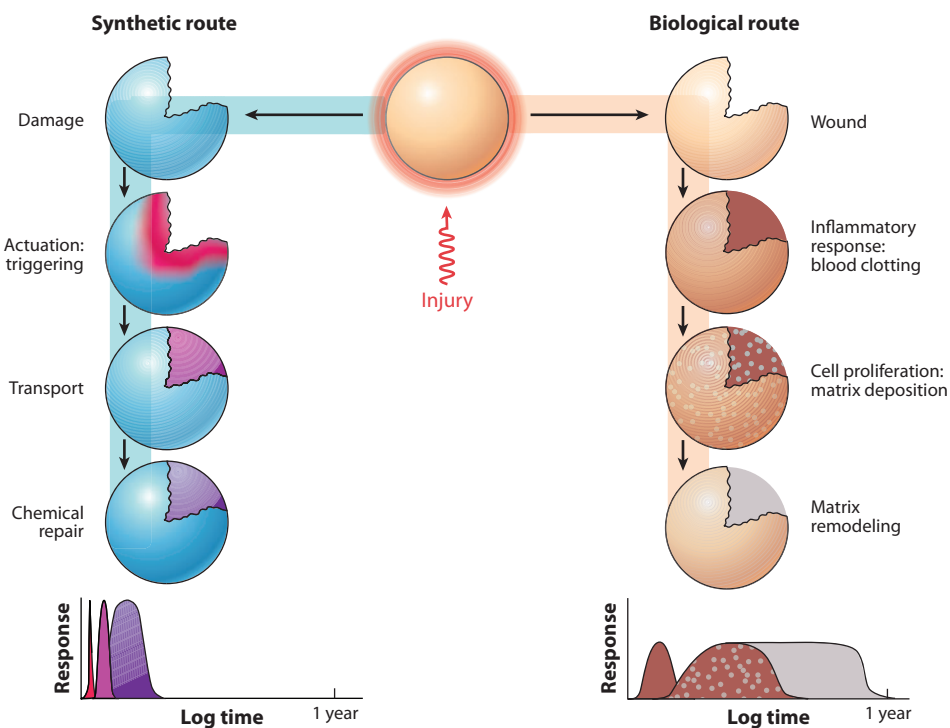
Figure 1

Synthetic and biological routes to healing. (*Right*) In biological systems, wound healing follows three sequential steps, the first of which is an immediate inflammatory response, including blood clotting. In the second stage, cell proliferation and matrix deposition occur and can extend for several days. The long-term response is matrix remodeling, which sometimes extends for several months. (*Left*) In synthetic materials, damage healing proceeds by an immediate response that actuates (triggers) the healing mechanism (e.g., the rupture of embedded microcapsules). Once triggered, the second stage involves transport of chemical species to the site of damage at a relatively rapid rate. During the final stage of healing, chemical repair takes place and can extend for several hours or days.

(actuation), which is closely coupled to the timescale of damage. The second response is transport of materials to the site of damage, again at a relatively rapid rate. The third response, analogous to matrix remodeling, is the chemical repair process, at a timescale that is dependent on the type of healing mechanism employed (e.g., polymerization, entanglement, reversible cross-linking).

The healing response is dictated by the kinetic rates of all three stages depicted in **Figure 1**: actuation, transport, and repair. The efficacy of healing is therefore regulated by the balance of the rate of damage versus the rate of healing (**Supplemental Figure 1**; follow the **Supplemental Material link** from the Annual Reviews home page at **http://www.annualreviews.org**). The rate of damage for a material is dictated by external factors such as the frequency of loading, strain rate, and stress amplitude. However, the rate of healing can be tailored or tuned to specific damage modes by, for example, varying the reaction kinetics through species concentration or temperature. Thus, the goal of self-healing is to achieve material stasis by balancing the rate of healing and the rate of damage.

The first overview of self-healing materials in 2007 (1) contained multiple chapters written by leading authorities in the field and covered the entire spectrum of materials from polymers to metals and ceramics. Since that time, several reviews and perspectives focused on self-healing polymers have appeared in the literature (2–11). Bergman & Wudl (2) described in detail intrinsic healing in polymers and their mechanisms. Wool's contribution (3) attempted to provide a general theory of damage and healing for polymers, drawing from the related field of polymer-polymer interfaces. Wu et al. (4) offered a primer on the fracture mechanics and mechanisms of healing in polymeric systems. The reviews by Kessler (5) and Yuan et al. (6) are more general and provide context for ongoing research in the field. In addition, a recent *MRS Bulletin* was devoted to self-healing polymers (7), with contributions summarizing self-healing chemistries (8), polymers (9), and composite systems (10). Trask et al. (11) also provided a recent perspective on self-healing fiber-reinforced composites (FRCs).

In this review article, we focus on self-healing polymers and fiber-reinforced polymer composites alone due to their relative maturity in comparison to ongoing research efforts in ceramics, metals, and other materials. We begin by describing the three primary self-healing conceptual approaches (capsule based, vascular, and intrinsic) and their demonstration in a variety of polymer systems as well as the critical issues and challenges associated with each approach. We then review the literature on self-healing under a variety of functional testing conditions, including resistance to fracture (quasi-static, fatigue, impact), recovery of barrier properties, and corrosion protection. We conclude the paper by discussing the future of self-healing polymers and composites—identifying new applications, functionalities, and material systems.

2. APPROACHES TO SELF-HEALING

Self-healing materials can be classified broadly into three groups: capsule based, vascular, and intrinsic (**Figure 2**). Each approach differs by the mechanism used to sequester the healing functionality until triggered by damage. The type of sequestration dictates the damage volume that can be healed, the repeatability of healing, and the recovery rate for each approach. This section presents an overview of the approaches that have been employed to prepare self-healing materials and of many of the relevant publications for each approach.

Capsule-based self-healing materials (**Figure 2a**) sequester the healing agent in discrete capsules. When the capsules are ruptured by damage, the self-healing mechanism is triggered through the release and reaction of the healing agent in the region of damage. After release, the local healing agent is depleted, leading to only a singular local healing event.

FRC: fiber-reinforced composite

Capsule-based healing: self-healing that utilizes healing agents sequestered in discrete capsules

Vascular healing: self-healing utilizing healing agents delivered to the damage by an embedded vascular network that has 1D, 2D, or 3D connectivity and may be replenished

Intrinsic healing: self-healing utilizing a latent material ability that is triggered by damage or an external stimulus such as heat, light, or pressure

Damage volume: the excess volume generated by material separation during damage. This volume requires filling for efficient healing after a damage event

▶ Supplemental Material
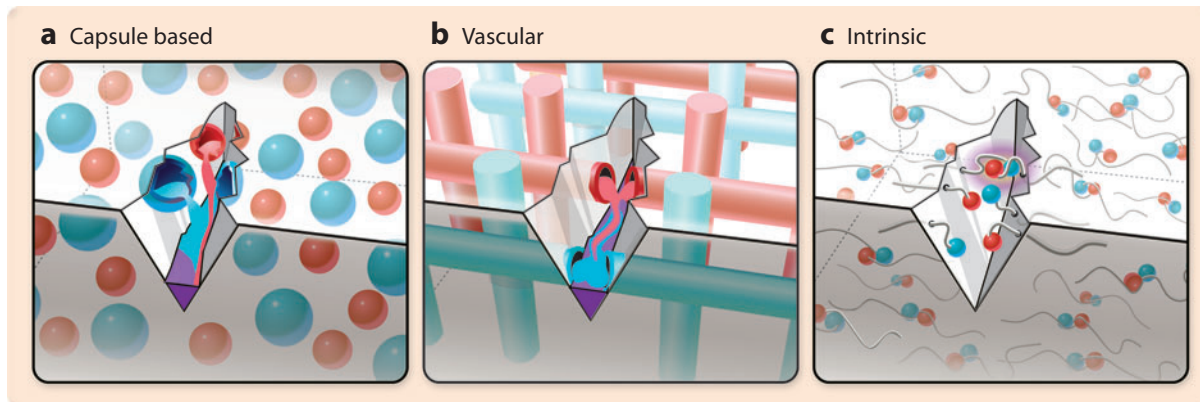
Figure 2

Approaches to self-healing include (*a*) capsule-based, (*b*) vascular, and (*c*) intrinsic methods. Each approach differs according to the method by which healing functionality is integrated into the bulk material. (*a*) In capsule-based self-healing materials, the healing agent is stored in capsules until they are ruptured by damage or dissolved. (*b*) For vascular materials, the healing agent is stored in hollow channels or fibers until damage ruptures the vasculature and releases the healing agent. (*c*) Intrinsic materials contain a latent functionality that triggers self-healing of damage via thermally reversible reactions, hydrogen bonding, ionomeric arrangements, or molecular diffusion and entanglement. Shades of red and blue are used in this figure and throughout the review to show a generalized interaction (*purple*) between two or more species.

Vascular self-healing materials (**Figure 2*b***) sequester the healing agent in a network in the form of capillaries or hollow channels, which may be interconnected one-dimensionally (1D), two-dimensionally (2D), or three-dimensionally (3D), until damage triggers self-healing. After the vasculature is damaged and the first delivery of healing agent occurs, the network may be refilled by an external source or from an undamaged but connected region of the vasculature. This refilling action allows for multiple local healing events.

Intrinsic self-healing materials (**Figure 2*c***) do not have a sequestered healing agent but possess a latent self-healing functionality that is triggered by damage or by an external stimulus. These materials rely on chain mobility and entanglement, reversible polymerizations, melting of thermoplastic phases, hydrogen bonding, or ionic interactions to initiate self-healing. Because each of these reactions is reversible, multiple healing events are possible.

2.1. Capsule-Based Self-Healing Materials

Capsule-based self-healing materials (**Figure 2*a***) sequester the healing agent in discrete capsules until damage triggers rupture and release of the capsule contents. In this section, a range of encapsulation techniques, the capsule-based material design cycle, and example capsule-based systems are described. Capsule-based self-healing systems are summarized in **Supplemental Table 1**.

2.1.1. Encapsulation techniques. A variety of techniques exist for encapsulation of reactive materials. These techniques can be classified as interfacial, in situ, coacervation, meltable dispersion, or physical on the basis of the mechanism of wall formation. A thorough description of these techniques is outside the scope of this review, but reviews of encapsulation techniques can be found in literature for food science, medical, industrial, and agricultural applications (12–14).

For self-healing materials, the most common encapsulation techniques are in situ, interfacial, and meltable dispersion. In situ and interfacial encapsulations proceed by reaction

Supplemental Material

of urea-formaldehyde (UF) (15–20), melamine-formaldehyde (MF) (21–23), melamine-urea-formaldehyde (MUF) (24), polyurethane (PU) (25), or acrylates (26) and the subsequent formation of a polymer shell wall at the interface of droplets in an oil-in-water (o/w) emulsion. Meltable dispersion encapsulations proceed by dispersion of the active core in a melted polymer. The melted polymer is emulsified to form droplets and solidified by temperature change or solvent removal to form a protective sphere around the core (27). Core-shell capsules have also been prepared by inverse emulsion (w/o) (28), Pickering stabilization (29), inverse Pickering stabilization (30), and multiple emulsions (31) in the literature but have not been used to date for self-healing materials.

2.1.2. Capsule-based self-healing material design cycle. The material design cycle, which is similar for each capsule-based self-healing materials scheme, is shown in **Figure 3b**. The design cycle can be broken into five steps: development, integration, mechanical characterization, triggering, and healing evaluation.

The first challenge is determining the optimal sequestration method for the healing agent and polymerizer. This sequestration can be achieved through encapsulation or phase separation. The main considerations for sequestration are the solubility, reactivity, viscosity, volatility, and pH of the material to be sequestered. Ideally, the core is oil soluble, is unreactive with the wall-forming chemistry, has low viscosity, and is nonvolatile. Although these properties describe the ideal healing agent for sequestration, alternate encapsulation methods may allow for sequestration of healing agents or polymerizers that do not meet these criteria.

After sequestration is achieved, the next consideration is integration. The shear forces induced on the capsules during mixing, processing temperature, capsule-matrix reactivity, and size scale of the capsules may vary. UF, MF/MUF, and PU capsules used for self-healing have shown an ability to survive processing conditions in common thermoset resin matrices and composite manufacturing processes and have been prepared at multiple size scales.

After the capsules are incorporated into the material, the mechanical properties, triggering mechanism, and healing performance can be characterized. The capsule bond strength with the matrix, the capsule volume fraction, and the capsule stiffness may affect mechanical properties of the self-healing material such as strength, fracture toughness, and elastic moduli. The triggering mechanism can be validated by observation of capsule rupture and release in situ or by postmortem observation of the release of core material on the crack plane, by optical microscopy of a fracture plane showing ruptured capsules, by infrared spectroscopy (IR), and even more conclusively by scanning electron microscopy (SEM) and energy-dispersive X-ray spectroscopy (EDS) of the fracture plane. Self-healing performance can be evaluated by various testing methods, depending on the intended application. For example, polymers and composites used in structural applications are assessed commonly by measuring fracture toughness, stiffness, or other mechanical properties. The healing performance of each self-healing system is dependent on damage volume, damage rate, healing rate, healing temperature, and bond strength between the healed material and the matrix material. Direct evidence of healing may also be observed postmortem by optical microscopy, IR, or SEM techniques.

2.1.3. Capsule-based self-healing. Capsule-based self-healing materials have been developed for some of the most commonly used synthetic polymers and elastomers using a variety of capsule-based sequestration schemes. Each scheme sequesters a healing agent in a discrete capsule until damage triggers release.

Figure 3a shows four schemes for sequestration of the healing agent. In the first scheme (capsule-catalyst), the healing agent is an encapsulated liquid, and the polymerizer is a dispersed catalyst phase (**Figure 3a**, *1*). An example capsule-catalyst system is the dicyclopentadiene

Fracture toughness: a material property quantifying the resistance to crack propagation in terms of a critical stress intensity factor
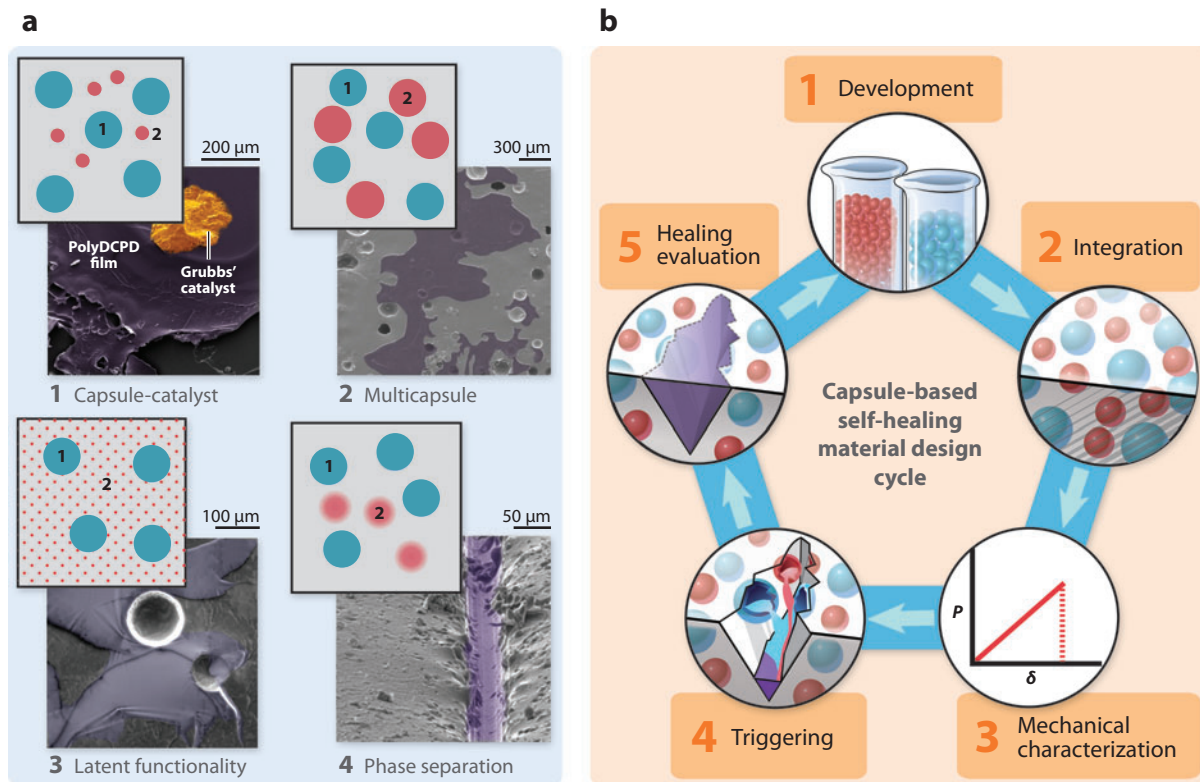
Figure 3

Capsule-based self-healing materials. (*a*) Capsule-based self-healing includes four main sequestration schemes. Materials with the sequestered components are labeled as *1* and *2*. (*1*) Capsule-catalyst systems include an encapsulated healing agent and a dispersed catalyst phase, an example of which is the dicyclopentadiene (DCPD)-Grubbs' capsule-catalyst system. Adapted from Reference 35 with permission from Elsevier. (*2*) Multicapsule systems utilize two or more capsules that sequester separate components of the healing agents, an example of which is the dual-capsule PDMS system. Adapted from Reference 18 with permission from Wiley-VCH. (*3*) Latent functionality systems make use of functional groups within the matrix phase that react with an encapsulated healing agent upon damage and release, an example of which is the epoxy-solvent system. Adapted from Reference 64 with permission from Wiley-VCH. (*4*) Phase-separated systems include at least one healing component that is phase separated within the matrix, whereas other components may be encapsulated. An example is the tin-catalyzed PDMS phase-separated system. Adapted from Reference 60 with permission from Wiley-VCH. (*b*) The design cycle for capsule-based self-healing materials is composed of (*1*) development of encapsulation/separation technique(s), (*2*) capsule integration into the bulk material, (*3*) characterization of mechanical properties, (*4*) validation of damage triggering and release of healing agents, and (*5*) evaluation of healing performance.

DCPD:
dicyclopentadiene

Healing efficiency:
a quantitative measure of the restoration and recovery of a lost or degraded property or performance metric

(DCPD)-Grubbs' first-generation catalyst system of White et al. (32). This system proceeds on the basis of the ring-opening metathesis polymerization (ROMP) of DCPD via the Grubbs' catalyst. In a series of papers describing autonomic self-healing using a UF-encapsulated DCPD healing agent and Grubbs' catalyst, Brown et al. reported high healing efficiencies (33), fatigue life extension (34, 35), and a significant quasi-static toughening effect (36). This DCPD-Grubbs' self-healing system has been incorporated into bulk matrices of epoxy (15, 32–40), fiber-reinforced epoxy composites (41–45), epoxy vinyl ester (46), and thermoplastic-elastomeric block copolymers (47). In addition, the DCPD-Grubbs' self-healing system and the mechanisms involved have been studied computationally (32, 48, 49). Wilson et al. (50, 51) examined various catalysts,

and Liu et al. (52) screened a variety of diene monomers for self-healing potential. Kamphaus et al. (53) explored the use of tungsten hexachloride (WCl_6), another ROMP catalyst, for improved thermal stability in self-healing epoxy, and Rule et al. (27) encapsulated Grubbs' catalyst in wax spheres via meltable dispersion to preserve catalyst activity. Moll et al. (41) developed a self-sealing composite by incorporating DCPD-filled capsules and wax-protected Grubbs' catalyst spheres into a glass fiber–reinforced epoxy composite. In a separate capsule-catalyst system, Rong et al. (54) incorporated epoxy resin–filled capsules in an epoxy matrix containing a thermally activated imidazole catalyst phase, and Yin et al. (55–58) extended this work to composite materials.

In the second sequestration scheme (multicapsule), both the healing agent and the polymerizer are encapsulated (**Figure 3a**, 2). This multicapsule technique can be expanded to include as many distinct capsule types as necessary to sequester the reactive components of the healing system. Keller et al. (18, 59) demonstrated multicapsule self-healing in an elastomeric matrix using two distinct capsule types, each filled with one part of the two-part Sylgard® 180 polydimethylsiloxane (PDMS). In this system, the healing reaction is a platinum-catalyzed hydrosilylation of vinyl-terminated PDMS resin (18). Cho et al. (60) extended PDMS multicapsule healing to corrosion inhibition by incorporating PDMS resin capsules and dimethyldineodecanoate tin (DMDNT) catalyst capsules in an epoxy coating, and Beiermann et al. (61) further extended the multicapsule PDMS system to a self-sealing laminated composite by dispersing encapsulated tin catalyst di-*n*-butyltin dilaurate (DBTL) and encapsulated PDMS resin in a PDMS matrix layer. Separately, Yuan et al. (21) developed a multicapsule system consisting of an encapsulated epoxide and an encapsulated mercaptan for healing in epoxy matrices. Xiao et al. (62) demonstrated self-healing based on cationic chain polymerization by inclusion of capsules containing boron trifluoride diethyl etherate [$(C_2H_5)_2O \cdot BF_3$] and epoxy resin–loaded capsules in an epoxy matrix.

In the third scheme (latent functionality), the healing agent is encapsulated or dispersed as particles, and the polymerizer is residual reactive functionality in the matrix or an environmental stimulus (**Figure 3a**, 3). An example of a latent system is the solvent-promoted and resin-solvent self-healing of Caruso et al. (63, 64). In this self-healing scheme, residual amine functionality in an epoxy matrix is utilized to initiate polymerization of the delivered healing agent. Zako & Takano (65) developed a separate system with latent functionality by incorporating thermally polymerizable, meltable, epoxy spheres into epoxy composite materials. Suryanarayana et al. (66) developed a latent system consisting of encapsulated linseed oil, which upon release and environmental exposure oxidizes to form a film to prevent corrosion damage. Kumar et al. (67) incorporated various healing agents in PU, acrylic, and other paints that, when released, reduced corrosion of a steel substrate. Sauvant-Moynot et al. (68) incorporated water-soluble self-curing epoxy-amine adduct particles in a protective film on a steel substrate. Exposure to an aqueous environment triggered the mobility of the epoxy-amine adduct to prevent corrosion. Grigoriev et al. (69) encapsulated benzotriazole, a corrosion inhibitor, into mesoporous SiO_2 particles and incorporated those particles into a sol-gel coating on an AA2024 aluminum alloy substrate.

In the fourth capsule-based scheme (phase separation) for self-healing, either the healing agent or the polymerizer is phase-separated in the matrix material (**Figure 3a**, 4). Cho et al. demonstrated this concept by phase-separating hydroxyl end-functionalized polydimethylsiloxane (HOPDMS) and polydiethoxysiloxane (PDES) in a matrix of epoxy vinyl ester to restore mechanical integrity (25) and to prevent corrosion (60). In these systems, the tin catalysts (DBTL/DMDNT) were encapsulated for protection until matrix damage triggered their release and catalyzed the reaction with the phase-separated HOPDMS/PDES.

Self-sealing: self-healing for the restoration of barrier properties, i.e., prevention of fluid diffusion across the material thickness, providing a seal

2.2. Vascular Self-Healing Materials

Vascular self-healing materials (**Figure 2***b*) sequester the healing agent in a network in the form of capillaries or hollow channels, which may be interconnected until damage triggers self-healing. In this section, vascular network fabrication, the vascular material design cycle, and example vascular self-healing systems are described. A summary of vascular systems is presented in **Supplemental Table 2**.

2.2.1. Vascular material design cycle. The design cycle for vascular networks (**Figure 4***b*) can be partitioned in a manner similar to capsule-based healing systems. Many of the same issues must be considered with regard to mechanical characterization, the triggering mechanism, and the healing performance. Where the two systems differ is with respect to fabrication and integration within a matrix material. Depending on the fabrication method, the interactions between the matrix materials, the healing agents, and the network materials play a crucial role in the effective development of a self-healing system.
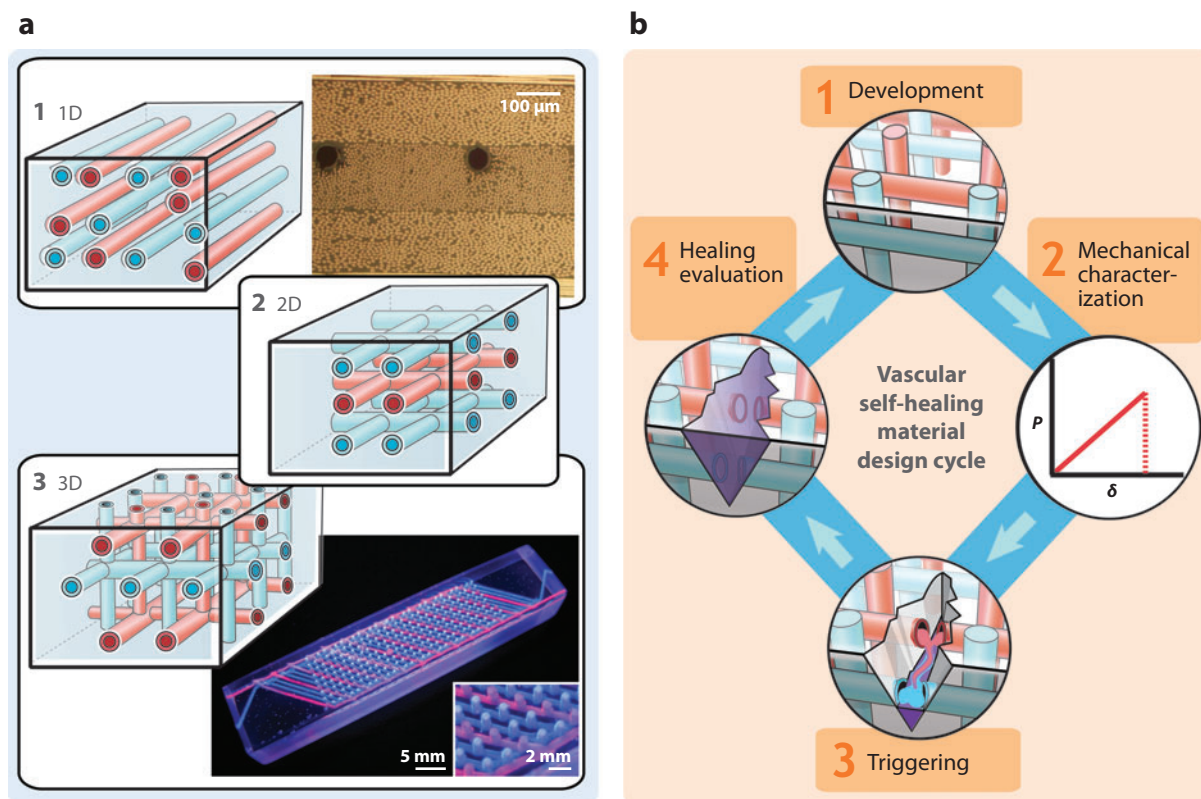
Figure 4

Vascular self-healing materials. (*a*) Vascular self-healing is organized according to the connectivity of the vascular network. (*1*) One-dimensional (1D) networks are obtained from hollow channels/fibers filled with healing agent(s), an example of which is the carbon fiber/epoxy laminate with hollow glass fibers containing a two-part epoxy healing agent. Adapted from Reference 78 with permission from Elsevier. (*2,3*) Two- and three-dimensional (2D and 3D) networks require more sophisticated manufacturing to ensure connectivity. An example of 3D connectivity is the interpenetrating networks containing a two-part epoxy healing agent manufactured using direct-write assembly. Adapted from Reference 92 with permission. (*b*) The design cycle for vascular self-healing materials includes (*1*) development of manufacturing and integration techniques, (*2*) characterization of mechanical properties, (*3*) validation of damage triggering and release, and (*4*) evaluation of healing performance.

The literature discusses two main techniques used for the assembly of network structures for self-healing. The first is to employ hollow glass fibers (HGFs) as channels (∼60 μm), filled with the appropriate healing agent (**Figure 4a**). HGFs are easily made using existing glass fiber drawing techniques, are compatible with many standard polymer matrices, and are inert to many popular self-healing agents such as two-part epoxy resin systems and cyanoacrylates. In addition, these fibers can be integrated into glass and carbon fiber plies for use in composites due to their similar size and shape. Although self-healing networks made from these fibers enjoy a number of advantages in terms of practicality, they are restricted to 1D connectivity.

For vascular systems, additional connectivity adds numerous performance advantages. Any location in the network has multiple connection points, leading to increased reliability with regard to channel blockages and a larger accessible reservoir for the healing agent(s). Multiple connections between channels also allow for easier refilling of the network after depletion. The technique used most commonly for higher-connectivity vascular fabrication is direct-ink writing of a fugitive ink scaffold and subsequent infiltration with an uncured polymeric precursor. The scaffold is subsequently removed after solidification, leaving a hollow channel network embedded with the polymer matrix. This technique provides control over network shape and connectivity but restricts the choice of matrix to materials that can be formed around the fugitive scaffold. The literature discusses other methods for creating networks with 3D connectivity, such as melt-spun sugar scaffolds or selective matrix disintegration via rapid electrical discharge (70), but such methods have yet to be applied to self-healing systems.

As opposed to capsule-based systems, for vascular materials the healing agents are introduced after the network has been integrated into the matrix. Thus, some properties that determine the choice of healing agents are surface wettability, chemical reactivity, and viscosity. High viscosities and/or unfavorable wetting properties prevent efficient filling of the network, whereas chemical incompatibility endangers long-term stability of the system. These properties also affect vascular network design, especially the channel diameter, because viscosity and wettability affect the release and transport of the healing agent(s).

The mechanical properties of a matrix with an embedded network are affected by the network wall stiffness, the bonding between the matrix and the network, the network volume fraction, and channel distribution and uniformity. The triggering mechanisms are validated and the healing performance characterized in a manner similar to capsule-based systems. Importantly, for vascular healing systems, access to a large reservoir of healing agent(s) and the ability to replenish the network enable repeated healing of multiple damage events.

2.2.2. One-dimensional networks. Dry and coworkers (71, 72) carried out initial investigations into self-healing 1D systems. The researchers qualitatively examined the healing ability of epoxies with millimeter-diameter glass pipettes preloaded with either cyanoacrylate or a separated two-part epoxy system. Motuku et al. (73) further explored the use of pipettes, along with tubes made of several different materials, to evaluate their suitability for incorporation into fiber-reinforced vinyl ester and epoxy resins. The researchers examined the network volume fraction and specimen thickness effects on matrix impact response but did not evaluate the healing ability of the networks.

Commercially available 15-μm-diameter HGFs were adopted by Bleay et al. (74) and were organized into unidirectional plies for composite laminates. Fibers within cured laminate specimens were filled with various fluids using applied vacuum, and release from fibers into damage zones was observed by ultrasonography and X-radiography. Pang & Bond (75, 76) fabricated 60-μm-diameter HGFs for more effective fluid filling and incorporated both HGF plies and solid glass fiber plies into a hybrid laminate. These authors tested a two-part epoxy resin system, with

HGF: hollow glass fiber

the healing components sequestered in separate HGF layers oriented in an orthogonal pattern. Bond and coworkers further explored the structural effects of channel integration on FRCs by fabricating quasi-isotropic $[0°/\pm 45°/90°]_S$ specimens with HGFs at the $(-45°/0°)$ ply interfaces (**Figure 4a**, *1*) and by subsequently filling them with a premixed two-part epoxy healing system (77, 78) or the individual components of a two-part epoxy healing system (77, 79).

2.2.3. Two- and three-dimensional networks. Williams et al. (80) examined several aspects of vascular networks, including the effects of channel diameter on optimized fluid flow. The researchers also looked at likely network failure modes (81) such as channel blockage restricting access to a damage site and large-scale leakage from fractured channels. Reliability strategies to guide future designs are inspired by biological circulatory models covering network redundancy, channel size restrictions, flow segregation, and fluid replenishment.

Networks with 2D connectivity may act as useful intermediates between discrete channels and 3D networks. For many composite matrices assembled by stacking unidirectional plies, 2D networks should integrate favorably at the interface between plies (**Figure 4a**, *2*), reducing any adverse impact on mechanical strength while maintaining an increased degree of interconnectivity. Bejan and coworkers (82–85) modeled 2D interconnected networks to optimize matrix coverage, fluid pumping power required, and reliability through choices of channel diameter, network shape, and network connectivity. Williams and coworkers (86, 87) constructed self-healing 2D networks within composite sandwich panels. The authors assembled a hierarchical network containing the components of a two-part epoxy system, with polyvinyl chloride tubes acting as major vessels in the panel midplane and smaller channels drilled normal to those channels to extend through the foam core, terminating at the composite skin.

Aragón et al. (88) created a modeling and optimization scheme for designing 3D networks based on genetic algorithms, using various network properties such as reliability, channel diameter, and network volume. Toohey et al. (89, 90) used direct-ink writing to produce 3D vascular self-healing epoxy mimicking the structure and functionality of epidermal tissue. In this work, a brittle epoxy coating with Grubbs' catalyst incorporated was deposited on a flexible epoxy substrate containing a 3D grid network of microchannels ($\sim$200 μm) containing a DCPD monomer healing agent. Surface cracks in the coating released DCPD from the underlying vascular substrate, which subsequently polymerized upon contact with the catalyst in the coating. The interconnected nature of the vascular network was exploited to refresh the reservoir of monomer and to heal samples repeatedly for up to seven consecutive cycles. To extend the number of healing cycles, Toohey et al. (91) adopted a two-part epoxy healing chemistry, using isolated networks to hold each component. This extended the number of repeated healing cycles to 16. Hansen et al. (92) refined direct-ink writing methods to make complex, isolated interpenetrating networks (**Figure 4a**, *3*) in order to optimize stoichiometry and to improve mixing for a two-part epoxy healing system and have achieved more than 30 repeated healing cycles.

2.3. Intrinsic Self-Healing Materials

Intrinsic self-healing materials (**Figure 5**) achieve repair though inherent reversibility of bonding of the matrix polymer. Intrinsic self-healing can be accomplished through thermally reversible reactions, hydrogen bonding, ionomeric coupling, a dispersed meltable thermoplastic phase, or molecular diffusion. In this section, we describe the intrinsic self-healing material design cycle and example intrinsic self-healing systems. A summary of intrinsic systems is presented in **Supplemental Table 3**, and further details on the historical development and synthesis of many of these polymers are available in a review by Bergman & Wudl (2).
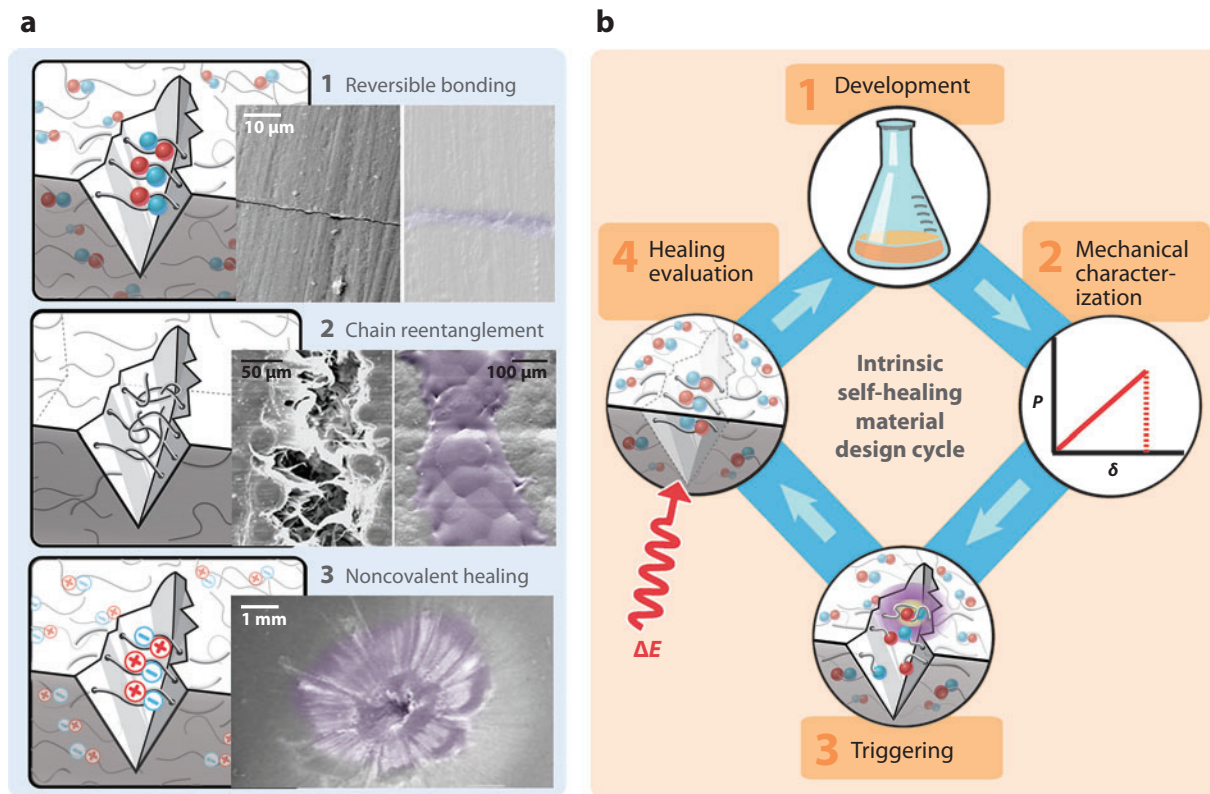
Figure 5

Intrinsic self-healing materials. (*a*) Intrinsic self-healing materials have been demonstrated using three main schemes. (*1*) Reversible bonding schemes make use of the reversible nature of certain chemical reactions that have been adapted to self-healing applications, an example of which is the Diels-Alder–retro-Diels-Alder healing system. Reprinted in part from Reference 98 with permission from the American Chemical Society. (*2*) Chain entanglement approaches utilize mobility at crack faces to entangle chains that span the crack surfaces, an example of which is the self-healing epoxy containing phase-separated poly(caprolactone). Reprinted in part and adapted from Reference 102 with permission from the American Chemical Society. (*3*) Noncovalent self-healing systems rely on reversible hydrogen bonding or ionic clustering that manifests as reversible cross-links in polymers, an example of which is the poly(ethylene-*co*-methacrylic acid) (EMAA) self-healing ionomer. Reprinted and adapted from Reference 105 with permission from Elsevier. (*b*) The design cycle of intrinsic materials is composed of (*1*) matrix material development, (*2*) mechanical characterization of the material, (*3*) validation of triggering, and (*4*) evaluation of healing performance, typically with the intervention of external energy.

2.3.1. Intrinsic self-healing material design cycle. The design cycle of intrinsic self-healing materials is less complex than that of capsule-based and vascular self-healing materials (**Figure 5*b***). For intrinsic systems, the matrix is inherently self-healing, and sequestration of healing agents is no longer required, avoiding many of the problems with integration and healing-agent compatibility that arise in vascular and capsule-based self-healing materials. However, intrinsic self-healing materials must also meet the desired mechanical, chemical, and optical properties for intended applications. Healing performance can be evaluated using the same protocols used for capsule-based and vascular approaches.

2.3.2. Self-healing polymers based on reversible reactions. Self-healing materials based on reversible reactions include components that can be reversibly transformed from the monomeric

state to the cross-linked polymeric state through the addition of external energy (2). Generally, a damaged polymer is subjected to heat or intense photoillumination, triggering enhanced mobility in the damage region, bond reformation, and polymer remending (**Figure 5a**, *1*). The most widely used reaction scheme for remendable self-healing materials is based on the Diels-Alder (DA) and retro-Diels-Alder (rDA) reactions. Chen et al. (93, 94) demonstrated a thermally activated self-healing system based on the DA reaction of synthesized furan-maleimide polymers. Plaisted & Nemat-Nasser (95) demonstrated increased healing efficiency and the repeatable healing of a similar furan-maleimide polymer. Park et al. utilized the DA reaction to incorporate healing functionality in a novel polymer derived from cyclopentadiene and characterized this derivative both as a bulk matrix (96) and as the matrix in a carbon fiber composite (97). Murphy et al. (98) developed and tested another cyclopentadiene derivative capable of multiple thermal remending cycles. To demonstrate DA reaction–based self-healing in a thermoset epoxy matrix, Peterson et al. (99) dispersed particles of a furan-maleimide gel as a secondary phase in an epoxy-amine matrix to trigger self-healing upon thermal activation.

2.3.3. Self-healing from dispersed thermoplastic polymers. Self-healing in thermoset materials can be achieved by incorporating a meltable thermoplastic additive. Self-healing occurs by the melting and subsequent redispersion of the thermoplastic material into the crack plane, filling the crack and mechanically interlocking with the surrounding matrix material (**Figure 5a**, *2*). Hayes et al. (100, 101) showed that incorporation of a dispersed thermoplastic resin, linear poly(bisphenol-A-coepichlorohydrin), into an epoxy composite reduced delamination area, eliminated matrix cracking, allowed for recovery of load bearing after thermal healing, and allowed for multiple healing cycles. Luo et al. (102) prepared a thermally remendable thermoset epoxy resin by dispersing phase-separated poly(caprolactone) (PCL) in an epoxy matrix. Upon heating, the PCL melts and undergoes a volumetric thermal expansion to fill the damage.

2.3.4. Ionomeric self-healing materials. Ionomeric copolymers are a class of materials with ionic segments that can form clusters that act as reversible cross-links (**Figure 5a**, *3*). These clusters can be activated by external stimuli such as temperature or ultraviolet (UV) irradiation. Because the formation of the clusters is reversible, multiple local healing events are possible. Projectile testing of poly(ethylene-*co*-methacrylic acid) (EMAA) copolymers with ionic segments was conducted by Kalista et al. (103, 104) and investigated further by Varley & van der Zwaag (105, 106) (**Figure 5a**, *3*). The heat generated during projectile damage served as the trigger for self-healing in these cases.

2.3.5. Supramolecular self-healing materials. Polymers can be designed to form strong end-group and/or side-group associations via multiple complementary, reversible hydrogen bonds, resulting in a self-healing elastomeric polymer. Cordier et al. (107) demonstrated self-healing of a rubbery material prepared via supramolecular assembly, and Montarnal et al. (108) developed a simplified synthesis for the precursor molecules for the same system. After these rubbery self-healing materials are damaged, the pieces may be brought back into close contact to allow for reformation of the hydrogen bonds.

2.3.6. Self-healing via molecular diffusion. An alternate method for achieving intrinsic self-healing is molecular diffusion. O'Connor & Wool (109, 110) and McGarel & Wool (111) investigated the mechanisms involved in healing of damage in styrene-isoprene-styrene block copolymers and polystyrene. The healing phenomena for these polymers were time dependent and temperature dependent and occurred via void closure, surface interaction, and molecular entanglement

between the damaged faces. Yamaguchi et al. (112, 113) demonstrated self-healing via molecular diffusion and entanglement of dangling chains in a weak PU gel. Rahmathullah et al. (114) promoted molecular diffusion through thermal treatment of an epoxy matrix with excess amine functionality.

In addition to healing damage, molecular diffusion can inhibit corrosion. Aramaki (115) coated a zinc cathode with solutions of $CeCl_3$ inhibitor and a polymer layer. Andreeva et al. demonstrated self-healing barrier properties of polyelectrolyte multilayer (PEM) coatings made from alternating layers of poly(ethyleneimine) (PEI) and poly(styrene sulfonate) (PSS) (116) or PEI and PSS complexed with 8-hydroxyquinoline (8HQ) (117). When immersed in a corrosive environment, both types of PEM coatings prevented corrosion near scratch damage. Yabuki and coworkers examined fluoro-organic compounds as healing coatings for aluminum (118) and zinc (119), with self-healing triggered by increased mobility of the fluoro-organic compounds as the pH increased during cathodic corrosion.

3. ASSESSMENT OF HEALING PERFORMANCE

The goal of self-healing is to recover lost or degraded function due to damage in a material system. Complete filling of damage volume and reforming bonds across damage surfaces can restore fracture properties, but other types of functions can be healed as well. Researchers have studied the recovery of barrier properties to prevent leakage of a fluid (gas or liquid) across the material thickness or corrosion protection of a coated substrate. The assessment of healing performance for these areas is reviewed in the following sections.

The damage modes in polymers and polymer composites causing loss of function vary depending on the external stimuli. **Figure 6** depicts a range of possible damage modes in a polymer composite due to, e.g., impact, fatigue, fracture, puncture, and corrosion. For example, impact loading can lead to surface cracking, subsurface delamination, polymer matrix cracking, and transverse ply cracking, which taken together can severely affect mechanical and barrier properties. The damage volume depends on the loading conditions, the geometry, and the undamaged material properties.

To quantify healing, researchers have proposed multiple definitions of healing efficiencies. For convenience, we define healing efficiency (η) as a ratio of changes in material properties as

$$\eta = \frac{f_{HEALED} - f_{DAMAGED}}{f_{VIRGIN} - f_{DAMAGED}},$$
1.

where f is the property of interest.

Figure 7 summarizes the general capabilities of current self-healing approaches on the basis of estimates from the literature in terms of healing efficiency (as defined in Equation 1), damage volume, and the ratio of healing rate to damage rate (see **Table 1** for detailed quasi-static results). The goal of any self-healing system is 100% healing efficiency, and each self-healing approach has at least one example system that has achieved this goal. However, as evident in **Figure 7a**, the range of damage volumes that can be healed differs for each approach. Most intrinsic systems require small damage volumes for efficient healing because intrinsic rebonding requires close proximity of the damaged surfaces. Capsule-based systems can fill small to moderate damage volumes, given a limited capsule volume fraction. Vascular systems can deliver a healing agent to both small and large damage volumes, with the lower limit set by damage size that is large enough to intersect the vascular network. Given that vascular networks can be replenished, we speculate that the upper limit far exceeds the limit of capsule-based systems. As stated above, an optimal self-healing system recovers at the same rate that damage occurs to maintain material stasis. The vast majority
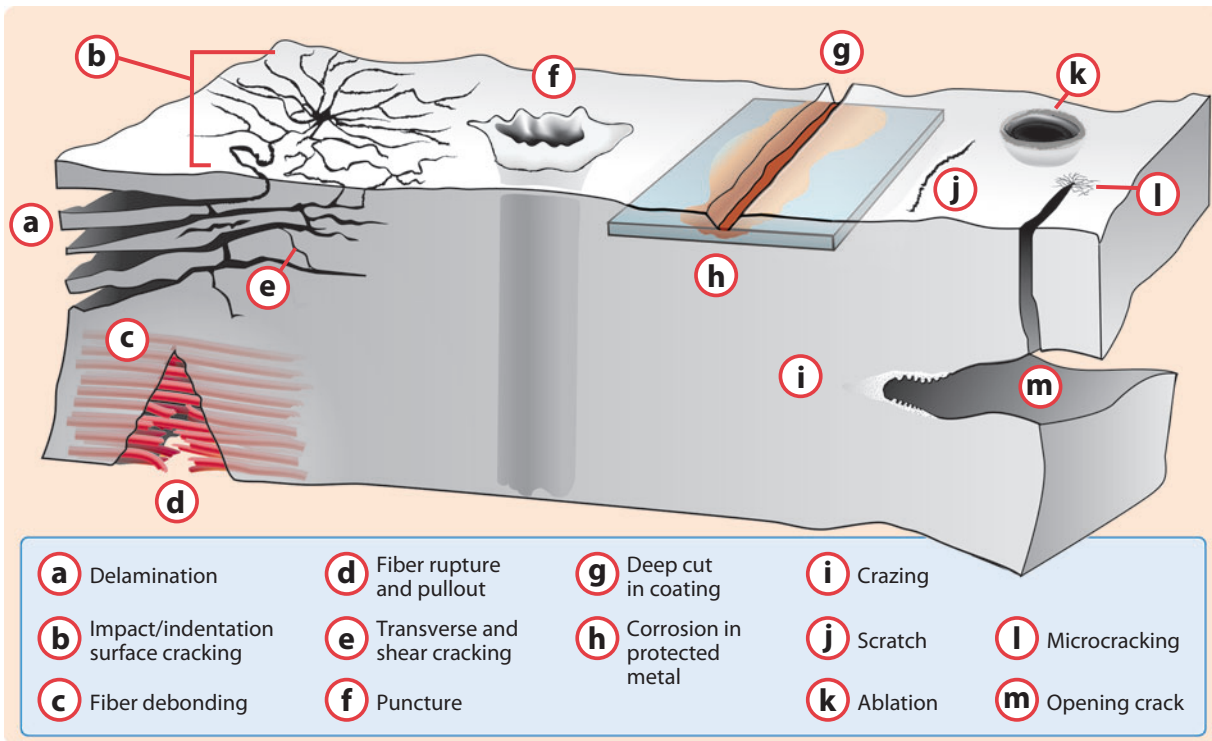
Figure 6

Damage modes in polymer composites. Indentation, impact, corrosive environments, ballistic punctures, surface scratching, and fatigue can lead to various damage modes in polymer composites, as shown here: (*a*) delamination, (*b*) impact/indentation surface cracking, (*c*) fiber debonding, (*d*) fiber rupture and pullout, (*e*) transverse and shear cracking, (*f*) puncture, (*g*) deep cut in coating, (*h*) corrosion in protected metal, (*i*) crazing, (*j*) scratch, (*k*) ablation, (*l*) microcracking, and (*m*) opening crack. The type of composite system, the nature of the polymer matrix, and the extent and rate of loading all influence the type and extent of damage modes that require healing. Self-healing systems have demonstrated significant healing of many of these damage modes, yet some, such as fiber breakage and ablation, have not been addressed to date.

of current self-healing systems are unable to match healing rate and damage rate (see **Figure 7**). Notable exceptions that achieve stasis are a capsule-based system from Brown et al. (35, 120), which indefinitely extended the fatigue life of epoxy for low applied stress intensity factors, and an intrinsic self-healing polymer from Kalista et al. (103), which sealed ballistic damage immediately after puncture.

3.1. Recovery of Fracture Properties

Damage in polymers and composites often involves some form of fracture, and for structural applications the recovery of fracture properties is an important research area. The primary fracture loading conditions for self-healing specimens have been quasi-static fracture, fatigue, and impact, as shown in **Figure 8**. These loading conditions cause several types of fracture, including Mode I crack opening, Mode III tearing, mixed-mode cutting, matrix-fiber delamination, and transverse (shear) cracking. Due to the scope of this review and the breadth of research in fracture studies, only some systems can receive detailed discussion here, with other systems more briefly mentioned for completeness.
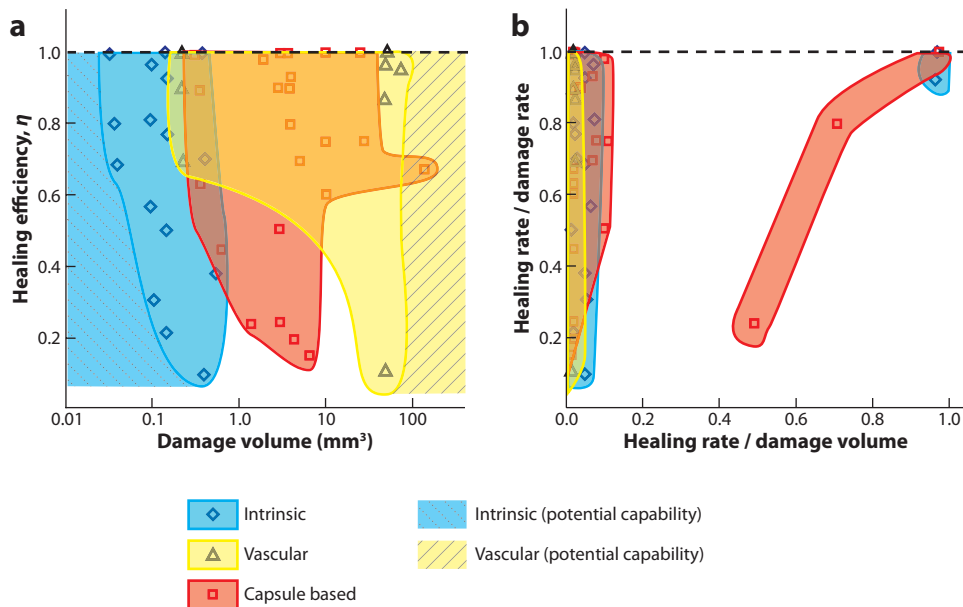
Figure 7

Performance maps for self-healing materials. The data are organized according to the type of self-healing with shaded regions on the basis of data in the literature (plotted as *discrete points*). (*a*) Each approach has demonstrated healing for different damage volume regimes. Intrinsic systems are relegated to small damage and can potentially heal at the molecular scale. Vascular systems have healed much larger damage volumes and can potentially extend the upper limit for self-healing systems. Capsule-based systems span the gap between intrinsic and vascular approaches. (*b*) Most systems have been demonstrated at low healing-rate-to-damage-rate ratios, regardless of approach. A few exceptions have achieved a balance between healing and damage rates and thus the desired material stasis.

3.1.1. Quasi-static fracture. In **Table 1**, we present a summary of self-healing polymer systems tested via quasi-static fracture methods. Quasi-static fracture experiments are common in the development of self-healing polymer systems because they allow for controlled, predictable crack propagation, often with small damage volumes and quantifiable fracture parameters. Damage volume depends on specimen geometry and the magnitude of applied force during the healing cycle. For quasi-static fracture, healing efficiency (η) reduces to the ratio of healed and virgin fracture properties because the fracture resistance in the damaged state is zero. Mode I fracture specimen geometries in self-healing research include double-cantilever beam (DCB), tapered double-cantilever beam (TDCB), compact tension (CT), single-edge notched beam (SENB), three-point bend, four-point bend, and double cleavage drilled compression (DCDC). Mode III tearing is induced through the trouser tear test for measuring tear strength. Cutting with a sharp blade leads to a complicated mixed-mode stress state around the cut edge and does not provide quantitative fracture data.

3.1.1.1. Mode I fracture of polymers. Epoxy-based systems have received the most attention in self-healing quasi-static Mode I fracture experiments. The first successful autonomic self-healing in a thermoset epoxy resin was by White et al. (32), demonstrating 75% recovery of virgin fracture toughness of TDCB specimens with a DCPD-Grubbs' catalyst capsule-based healing system. The tapered geometry of the TDCB specimen, which was first introduced by Mostovoy et al. (121),

TDCB: tapered double-cantilever beam

Table 1   Self-healing polymer systems under quasi-static fracture[a]

Material	Healing approach	Chemistry/method	Loading condition	Healing measure	Maximum healing efficiency (%)	Reference(s)
Epoxy/epoxy sphere phase/glass FRC	Capsule based	Meltable epoxy spheres	Mode I three-point bend	Peak fracture load	100	65
Mendomer 401/carbon FRC	Intrinsic	DA-rDA reaction	Mode I three-point bend	Strain energy	94	97
Epoxy	Vascular	DCPD-Grubbs'	Mode I four-point bend	Fracture toughness	38–70	89, 90
Epoxy	Vascular	Two-part epoxy	Mode I four-point bend	Fracture toughness	89–100	91, 92
2MEP4F polymer	Intrinsic	DA-rDA reaction	Mode I CT	Fracture toughness	83	94
Epoxy/thermoplastic phase	Intrinsic	Meltable secondary additive	Mode I CT	Fracture toughness	77	101
Epoxy	Intrinsic	Molecular diffusion of residual functionality	Mode I CT	Peak fracture load	68	114
2M4F polymer	Intrinsic	DA-rDA reaction	Mode I CT	Fracture toughness	57	93
Epoxy/furan-maleimide gel phase	Intrinsic	DA-rDA reaction of gel phase	Mode I CT	Peak fracture load	21	99
Epoxy/E-glass FRC	Capsule based	Epoxy–latent $CuBr_2(2\text{-MeIm})_4$ catalyst	Mode I DCB	Fracture toughness	68–79	55, 56, 58
Epoxy/E-glass FRC	Capsule based	DCPD-Grubbs'	Mode I DCB	Fracture toughness	60	44
2MEP4F polymer	Intrinsic	DA-rDA reaction	Mode I DCDC	Fracture toughness	100	95
Epoxy/PCL phase	Intrinsic	Meltable secondary additive	Mode I SENB	Peak fracture load	>100[b]	102
Epoxy	Capsule based	Epoxy–latent $CuBr_2(2\text{-MeIm})_4$ catalyst	Mode I SENB	Fracture toughness	111[b]	58
Polymers 400 and 401	Intrinsic	DA-rDA reaction	Mode I SENB	Fracture toughness	60	98
Epoxy	Capsule based	Epoxy-mercaptan	Mode I TDCB	Fracture toughness	104[b]	21
Epoxy	Capsule based	Solvent or epoxy resin solvent	Mode I TDCB	Fracture toughness	82–100	63, 64
Epoxy	Capsule based	DCPD-Grubbs'	Mode I TDCB	Fracture toughness	75–93	27, 32, 33, 36, 37
Epoxy/embedded SMA wires	Capsule based	DCPD-Grubbs'	Mode I TDCB	Fracture toughness	77	38, 40
Epoxy vinyl ester	Capsule based	DCPD-Grubbs'	Mode I TDCB	Fracture toughness	~30	46
Epoxy vinyl ester	Capsule based	PDMS-tin catalyst	Mode I TDCB	Fracture toughness	24	25

(*Continued*)

Table 1 (*Continued*)

Material	Healing approach	Chemistry/method	Loading condition	Healing measure	Maximum healing efficiency (%)	Reference(s)
Epoxy	Capsule based	DCPD-WCl$_6$ catalyst	Mode I TDCB	Fracture toughness	20	53
Epoxy/carbon FRC	Capsule based	DCPD-Grubbs'	Mode I WTDCB	Fracture toughness	80	42
Hydrogen-bonded molecules	Intrinsic	Noncovalent bonding: supramolecular	Mixed-mode cut	Visual	N/A[c]	107
Weak polyurethane gel	Intrinsic	Molecular diffusion	Mixed-mode cut	Visual	N/A[c]	113
PDMS	Capsule based	PDMS-Pt catalyst	Mode III tear test	Tear strength	115[b]	18
Weak polyurethane gel	Intrinsic	Molecular diffusion	Mode III tear test	Tear strength	80	112

[a]Abbreviations used: CT, compact tension; DA, Diels-Alder; DCB, double-cantilever beam; DCDC, double cleavage drilled compression; DCPD, dicyclopentadiene; FRC, fiber-reinforced composites; PCL, poly(caprolactone); PDMS, polydimethylsiloxane; rDA, retro-Diels-Alder; SENB, single-edge notched beam; SMA, shape memory alloy; TDCB, tapered double-cantilever beam; WTDCB, width-tapered double-cantilever beam.
[b]Reported healing is >100% because quantified healing measure in the healed case is greater than the virgin case.
[c]Qualitative healing capability is based on visual observation of the crack healing or on the ability of healed polymer to deform under tension.

allows for controlled crack growth along the centerline and a crack length–independent fracture toughness that depends only on the applied load. This feature of the TDCB allows for accurate evaluation of healing efficiency because the healed crack length is difficult to measure in situ.

Subsequent studies of epoxy TDCB specimens with DCPD-Grubbs' catalyst capsule-based healing examined the effects of microcapsules and of damage volume on fracture morphology, fracture toughness, and healing efficiency (27, 33, 36–38). Brown et al. (33, 36) determined that microcapsules increased the virgin toughness of epoxy. This toughening effect was attributed to the absorption of increased elastic energy via crack pinning, crack deflection, and microcracking (**Figure 8a**) (36). Through analysis of microcapsule size and concentration and the damage volume of TDCB specimens, Rule et al. (37) considered the vital role of damage volume in the design of a self-healing system, observing that the damage volume dictates the minimum volume of healing agent(s) required for optimal healing.

Several intrinsic self-healing epoxy systems highlight the importance of small damage volume achieved by small crack separation in Mode I specimens. The thermally remendable system from Luo et al. (102) was evaluated via three-point bend of SENB specimens. For this ductile system, the two crack faces could be rejoined upon unloading, and the damage volume was small enough for efficient healing. Hayes et al. (101) reported that a likely cause of variability in the healing efficiencies of their epoxy matrix–thermoplastic particle–blend CT specimens was the inconsistency of clamping pressures applied to the halves of the fully fractured specimens. Rahmathullah et al. (114) adopted a CT geometry modified with a crack arrest point to prevent complete fracture of the epoxy specimen to allow precise realignment of the crack faces before thermal and pressure treatment. The role of the clamping pressure was investigated, and the healing efficiency was found to increase with higher applied pressure.

Multiple healing cycles have been reported for several epoxy-based material systems. TDCB studies from Caruso et al. (63, 64) of solvent microcapsules in epoxy demonstrated multiple healing

Quasi-static fracture
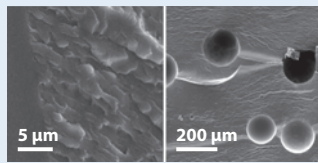
a TDCB Mode I plane

b DCDC Mode I

Top view

Side view

c Mixed-mode cutting

3 mm → 10 min → 3 mm

5 mm → 10 min → 5 mm

Healed virgin tear line

Second tear line

10 mm

Original tear line

300 μm
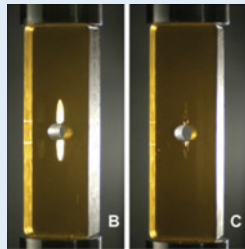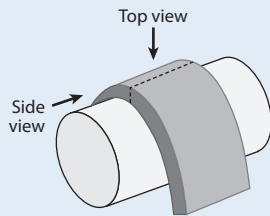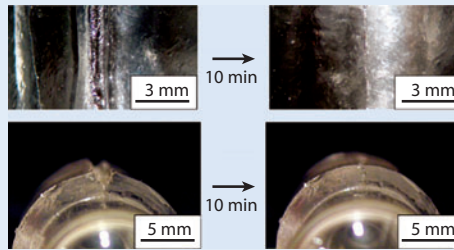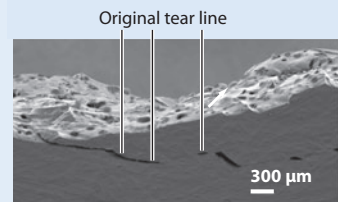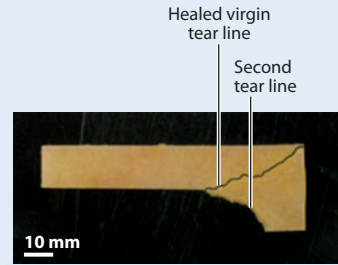
d Mode III tearing

Fatigue

500 μm   50 μm   5 μm
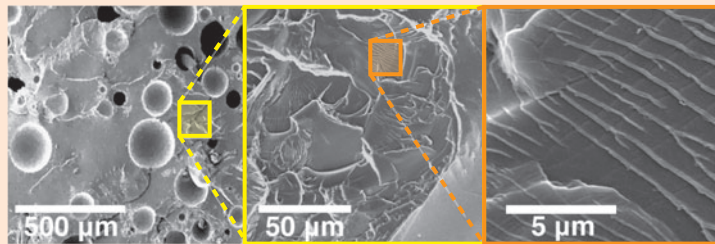
e TDCB Mode I fatigue crack plane morphology

Impact

f Mixed-mode damage

5 mm

100 μm

100 μm

1 mm

Indentation direction

Delamination

Microcracks

Fractured fibers
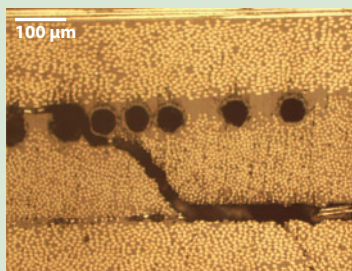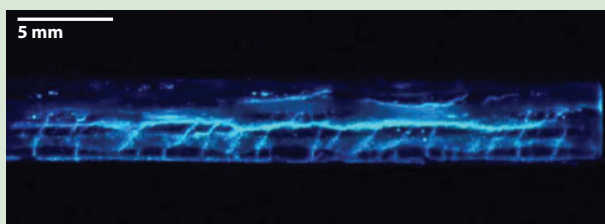
g Transverse and shear cracking
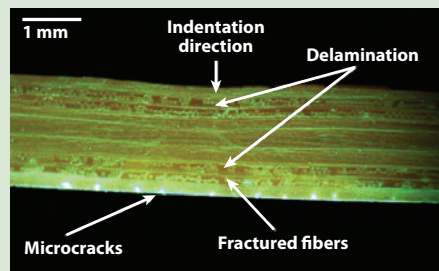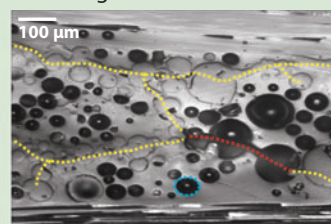
h Delamination

cycles whenever cracks deviated from the original virgin crack path. Healing efficiency decreased for each cycle as the local epoxy-solvent microcapsules and residual amines were depleted. Peterson et al. (99) used the modified CT geometry to study an epoxy matrix containing reversible cross-linked oligomer gel phases and showed multiple healing cycles at an elevated temperature of 90°C for 1 h followed by 12 h at room temperature under modest pressure.

Toohey et al. (89–91) introduced a bioinspired coating/substrate design that delivers a healing agent or multiple healing agents to cracks in a coating via a 3D microvascular network in the substrate. A DCPD monomer healing agent was stored in the embedded network, and a first-generation Grubbs' catalyst was incorporated into the coating. A single crack was introduced by four-point bending and healed up to seven times with a single, pervasive network (89). A maximum of 16 consecutive healing cycles was achieved by introducing a bicontinuous-network architecture for delivery of a two-part epoxy-based healing chemistry (91). Hansen et al. (92) improved this approach by creating interpenetrating microvascular networks capable of segregating a two-part epoxy healing chemistry while minimizing the separation between the two healing agents to facilitate mixing and stoichiometric balance in the damaged region, demonstrating more than 30 consecutive healing cycles in the process.

In addition to epoxy systems, quasi-static Mode I fracture studies have been conducted for epoxy vinyl ester and intrinsic thermally remendable polymers. A PDMS-tin catalyst capsule-based self-healing chemistry was used to create self-healing epoxy vinyl ester by Cho et al. (25) and was evaluated using TDCB fracture testing protocols. In this system, an 88% improvement in virgin fracture toughness was attributed to microcapsule toughening (25). Wilson et al. (46) utilized the DCPD-Grubbs' catalyst capsule-based approach to heal epoxy vinyl ester with modest healing efficiencies (∼30%) but with a healing efficiency higher than that of Cho et al. (∼24%).

Thermally remendable systems based on DA-rDA reactions have generally demonstrated recovery of Mode I fracture properties when the damage volume is small. Chen et al. (93) conducted CT testing of a synthesized furan-maleimide polymer (3M4F) and showed 50% recovery of the brittle fracture load in fully fractured specimens that were clamped together and heated at 150°C for 2 h for healing. Reduced healing efficiency was attributed to significant crack separation. To promote better registration of the CT crack faces, Chen et al. (94) next used a modified CT

Figure 8

Self-healing for recovery of fracture properties. Specific examples are grouped according to quasi-static fracture, fatigue, and impact loading conditions. (*a*) Scanning electron micrographs of crack plane morphology for a Mode I tapered double-cantilever beam (TDCB) self-healing epoxy specimen containing DCPD capsules and Grubbs' catalyst. Reprinted from Reference 36. (*b*) Optical images of Mode I crack growth in a double cleavage drilled compression (DCDC) intrinsic self-healing specimen based on the DA-rDA (Diels-Alder–retro-Diels-Alder) reversible bonding scheme. Stable crack growth (*left*) is healed (*right*) after 10 h at 85°C and 0.35-MPa clamping pressure and after 3 h at 95°C with no clamping pressure. Adapted from Reference 95. (*c*) Optical images of mixed-mode cutting (*left*) and healing (*right*) of an intrinsic self-healing polymer based on molecular diffusion and entanglement of dangling chains in a weak polyurethane gel. A polymer sample is stretched over a cylinder for viewing of crack damage and healed morphology. Adapted from Reference 113. (*d*) Optical image (*top*) and scanning electron micrograph (*bottom*) of a Mode III trouser tear self-healing polydimethylsiloxane (PDMS) specimen. Adapted from Reference 18. (*e*) Scanning electron micrographs of crack plane morphology for Mode I fatigue of a TDCB self-healing epoxy specimen containing DCPD capsules and Grubbs' catalyst. Adapted from Reference 120 with permission from Springer. (*f*) Ultraviolet (UV) and optical images of mixed-mode damage (*left*) and healing (*right*) due to impact in a woven glass fiber-reinforced composite (FRC) containing DCPD capsules and Grubbs' catalyst. Dashed yellow lines indicate healed delamination; dashed red line, unhealed delamination; dashed blue line, microcapsule. Adapted from Reference 43 with permission from Elsevier. (*g*) Optical micrograph showing transverse/shear cracking induced by impact loading in a carbon FRC with intermingled 60-μm hollow glass fibers (HGFs) containing a two-part epoxy healing agent. Adapted from Reference 78 with permission from Elsevier. (*h*) UV visualization of delaminations in glass FRC incorporating 60-μm HGFs containing a two-part epoxy healing agent. Adapted from Reference 75 with permission from Elsevier.

specimen geometry with a crack arrest hole to prevent complete failure of the specimen. In their study, a modified furan-maleimide polymer (3MEP4F) showed 80% recovery of fracture load after being clamped at 115°C for 30 min. Plaisted & Nemat-Nasser (95) studied the same 3MEP4F polymer, using a DCDC specimen (**Figure 8b**) in which two symmetric cracks emanating from the crowns of the central hole grew stably under compressive loading. The DCDC specimens were healed first at 85°C under 0.35-MPa normal pressure and then at 90°C under no pressure to encourage chain mobility. These specimens exhibited multiple healing cycles with full or close to full recovery of fracture toughness.

3.1.1.2. Mode I fracture of fiber-reinforced composites.

Initial studies of self-healing FRCs utilized quasi-static Mode I fracture experiments to examine the healing of interlaminar delamination. Kessler and coworkers (42) adopted a width-tapered DCB (WTDCB) of woven carbon FRCs with the DCPD-Grubbs' catalyst capsule-based self-healing system integrated into the epoxy matrix. Control specimens (without self-healing components) exhibited delamination along the midplane of the laminate as the primary damage mode and a stick-slip loading behavior during crack growth. Self-healing samples exhibited a reduction in virgin fracture toughness due to a thickening of the interlaminar region by the incorporated capsules (∼180 µm). After a 48-h healing period at room temperature, healing efficiencies of roughly 40% were achieved but increased to as much as 80% upon heating at 80°C. A woven E-glass FRC epoxy system from Yin et al. (55, 56, 58) containing a microencapsulated epoxy resin with latent hardener in the matrix demonstrated higher fracture toughness than did non-self-healing controls. Key factors precluding complete recovery of interlaminar fracture toughness were the lack of fiber bridging and the uneven distribution of healing agents on the fracture plane.

Preliminary assessment of healing in a carbon FRC containing an intrinsic thermally reversible self-healing matrix was conducted by Park et al. (97), using a three-point-bend testing protocol. Microcracks were healed by electrical resistive heating of the graphite fiber network to 150°C for 1 min, demonstrating more than 90% recovery of fracture energy for three healing cycles.

3.1.1.3. Mixed-mode cutting.

Qualitative evaluation of self-healing of fracture damage is often obtained by cutting a polymer sample and optically evaluating scratch damage and crack closure. The supramolecular polymer from Cordier et al. (107) was cut with a razor blade and allowed to heal for 15 min at room temperature following realignment of the cut pieces. Healed specimens could deform up to 200% compared with 500% for the virgin material. Yamaguchi et al. (113) showed that the intrinsic system of molecular diffusion of dangling chains in a weak PU gel was sufficient to heal cuts from a razor blade when fractured surfaces were brought back into contact and allowed to heal at room temperature for 10 min. Specimens showed no reopening of the crack faces when bent over a 12-mm-diameter cylinder for optical imaging (**Figure 8c**).

3.1.1.4. Mode III fracture.

Mode III fracture, via a trouser tear specimen, has been used to assess fracture recovery in self-healing samples. The PU gel of Yamaguchi et al. (112) showed restoration of 80% of the tear strength after 10 min at room temperature upon contact of the torn crack faces. Keller et al. (18) demonstrated 70–100% recovery of PDMS tear strength with a capsule-based PDMS-platinum catalyst healing system. In some tests of healed PDMS, the crack path deviated from the virgin crack path, as shown in **Figure 8d**, demonstrating full recovery of tear strength.

3.1.2. Fatigue.

Fatigue fracture is a common dynamic failure mode in structural materials and presents unique challenges to self-healing material design. Fatigue loading induces a damage rate

that depends on an array of variables, including the frequency and amplitude of the applied stress intensity factor and material mechanical properties. Healing rate is dependent on the kinetics of the self-healing approach, including temperature, mobility, and polymerization rates. A proposed measure of self-healing under fatigue loading is the fatigue life extension (λ) defined in terms of fatigue life (N) by Brown et al. (34, 35) as

$$\lambda = \frac{N_{HEALED} - N_{CONTROL}}{N_{CONTROL}}. \qquad 2.$$

To date, only a few studies of self-healing systems have considered fatigue damage. Zako & Takano (65) evaluated glass FRCs with an epoxy matrix containing embedded non-cross-linked epoxy beads. This capsule-based self-healing system demonstrated a fatigue life extension of $\lambda = 2$ for a tensile Mode I fatigue test incorporating a single unloaded thermal rest period of 120°C for 10 min after a 12.5% reduction in stiffness (65). Brown et al. (34, 35, 120), with modeling efforts from Maiti et al. (48, 49), considered Mode I fatigue of epoxy TDCB specimens with a DCPD-Grubbs' capsule-based self-healing system, showing varied fatigue life extension depending on the range of the applied stress intensity factor (ΔK_I). The addition of microcapsules improved resistance to fatigue crack propagation via fracture toughening mechanisms, evidenced by significant out-of-plane crack morphology at all length scales (**Figure 8e**), as well as hydrodynamic crack tip shielding and crack closure from polymerization of the healing agent. The DCPD-Grubbs' capsule-based system requires approximately 10 h for full healing (t_{heal}) (122). Thus, the time to fully fracture the specimen by fatigue (t_{fail}) must be greater than 10 h to observe life extension. For high $\Delta K_I = 0.7–0.9 K_{Ic}$ with $t_{fail} < t_{heal}$, where K_{Ic} is the Mode I fracture toughness, no life extension occurred unless a rest period of $t_{rest} = t_{heal}$ was inserted into the fatigue profile. For moderate $\Delta K_I = 0.5–0.7 K_{Ic}$ with $t_{fail} \sim t_{heal}$, the crack propagation slowed such that $\lambda = 0.89–2.13$. This system achieved infinite fatigue life extension (no crack extension over seven days) for smaller $\Delta K_I < 0.5 K_{Ic}$ and for the moderate ΔK_I case with one rest period of t_{heal}. For the same TDCB self-healing epoxy system, Jones et al. (39) greatly extended fatigue life by utilizing wax-protected Grubbs' catalyst, which increases the rate of polymerization by fourfold. In these cases, total crack arrest was achieved by matching the healing rate and the effective damage rate.

The PDMS-platinum catalyst capsule-based system from Keller et al. (59), in both Sylgard PDMS and RTV 630 PDMS matrices, produced significant torsional stiffness recovery with the specimens under Mode III torsional fatigue, ultimately reducing the total crack growth by 24%. Keller et al. proposed that the mechanisms for reducing crack growth include hydrodynamic crack tip shielding, crack closure, adhesive bonding, and increased friction between the rotating fracture planes due to the presence of polymerized healing agent in the crack plane. The time to the onset of recovery correlated with the bulk gel time of the healing agent, reinforcing the importance of balancing healing and damage kinetics for optimal healing.

3.1.3. Impact. Out-of-plane impact events can result in massive damage volume from several failure modes such as puncture, delamination, and mixed-mode cracking. Thus far, the focus of self-healing of impact-induced damage has been on healing of the polymer matrix in polymer composite panels subject to low-velocity impact. Healing has been quantified by restoration of compressive strength by compression-after-impact (CAI) testing.

Williams et al. (123) studied 2.6-mm-thick carbon FRC epoxy that incorporated 60-μm-diameter HGFs containing a premixed healing agent. Quasi-isotropic stacking sequences were considered with HGFs located at various ply interfaces. Panels were subject to a range of impact energies below 3 J for self-healing studies. In addition to the normal modes of energy absorption for composites subject to impact loading, the HGF system also absorbs significant energy as a

result of HGF fracture during impact, yielding a 13% increase in CAI strength in comparison to the strength of carbon FRC alone. CAI testing demonstrated significant healing of the composite with a two-step elevated temperature cure at 70°C for 45 min followed by 125°C for 75 min and also demonstrated sensitivity to the uniformity of channel distribution within the laminate. Williams et al. (86, 87) also studied a 2D vascular approach in sandwich composites with embedded 1.5-mm bore tubes (PVC or silicone) serving as arteries along the midplane and smaller channels extending vertically to the E-glass/913 epoxy laminated skins. Both a premixed system and an isolated, two-part epoxy healing system were evaluated using 3-J impact to induce damage and then edge compression to determine the skin compressive strength. Results for both the premixed resin and the two-part epoxy delivered at high pressure showed higher skin compressive strength than in the undamaged specimens. Results for the two-part epoxy healing delivered at low pressure showed only moderate recovery of the skin compressive strength above the damaged system.

Three other studies of self-healing epoxy composites subject to impact damage involve intrinsic or capsule-based healing approaches. Hayes et al. (100, 101) studied glass FRCs with an intrinsic self-healing epoxy matrix incorporating a thermoplastic additive. Charpy impact testing was carried out at 2.6 J of impact energy for three thermal healing cycles of 2 h at 130°C. However, the healing efficiencies quoted were calculated on the basis of the reduction of optically visible damage area and are difficult to compare with other published studies. Yin et al. (57) incorporated epoxy-filled microcapsules and a latent hardener in an epoxy matrix to heal woven glass FRC specimens after 1.5–3.5-J impacts. The authors calculated healing efficiencies (as defined in Equation 1) on the basis of recovery of compressive strength (σ) as

$$\eta_{CAI} = \frac{\sigma_{HEAL} - \sigma_{DAMAGED}}{\sigma_{VIRGIN} - \sigma_{DAMAGED}}$$ 3.

and reported close to 100% efficiency for 1.5-J impacts but only ∼20% efficiency for 3.5-J impacts. Patel et al. (43) demonstrated significant recovery of compressive strength for much higher impact energies (13–45 J) for 4-mm-thick woven glass epoxy FRCs with a DCPD-Grubbs' capsule-based healing system. Samples exhibited extensive delamination, transverse cracking, and matrix cracking, as visualized by fluorescently marked cracks in a damaged composite cross section and the optical image of a crack through an epoxy-rich region in **Figure 8f**. Healing efficiency was nearly 100% for impact energies up to 20 J and decreased with increased damage volume at higher impact energies.

3.1.4. Indentation. Indentation testing is a means to simulate impact failure mechanisms, but with less damage. Pang & Bond (75, 76) indented epoxy composites containing standard E-glass fiber plies and plies of 60-μm-diameter HGFs loaded with either epoxy resin (MY750 Ciba-Geigy + 30 wt% acetone) mixed with a UV fluorescent dye (Ardrox 985) or the corresponding hardener. HGF plies were oriented such that the resin fibers were aligned with 0° orientation and hardener fibers were orthogonal. Indentation experiments were carried out under load control up to 1200 N, yielding an equivalent impact energy of ∼0.5–0.6 J and resulting in delamination, matrix cracking, and fracture of the HGFs. Flexural testing of damaged and healed specimens demonstrated roughly 93% retension of flexural strength for a 24-h room temperature healing period (75). Four sets of specimens were aged zero, three, six, or nine weeks after fabrication to examine environmental stability of the systems (76). Compared with non-self-healing damaged specimens that retained 75% of the virgin flexural strength, the aged samples retained 93%, 75%, 78%, and 55% of the virgin flexural strength for the zero-, three-, six, and nine-week aging

conditions, respectively. Despite long-term storage issues, this healing system showed extensive release and infiltration of damage within laminates, as revealed in **Figure 8***b*.

A series of papers by Trask and coworkers (77–79) studied the flexural properties of glass and carbon FRC epoxy laminates incorporating HGF delivery of two-part epoxy healing agents. For E-glass/913 epoxy FRCs with HGF layers containing separate components of a Cycom 823 epoxy, indentation experiments were performed up to 2500-N loading to create extensive damage. The flexural strength after damage and prior to healing was 74% of an undamaged E-glass FRC and was 87% after healing for 2 h at 100°C (77, 79). Trask and coworkers (78, 79) then intermingled 60-μm-diameter HGF fibers within unidirectional carbon fiber plies. For carbon fiber/914 epoxy FRCs with HGF fibers intermingled, indentations were carried out at 1700–2000-N loading. Restoration of flexural strength was demonstrated when a premixed Cycom 823 epoxy was loaded into HGFs and a two-step healing period was followed: 45 min at 75°C followed by 75 min at 125°C. Delaminations sometimes deviated toward the HGF, causing HGF rupture and epoxy resin/hardener release. Transverse/shear matrix cracks were interconnected, creating a damage network that facilitated resin flow and infiltration (**Figure 8***g*).

The effect of HGF incorporation on virgin properties was also evaluated in these systems. For the E-glass/913 system with separate HGF plies, Trask and coworkers (79) observed a 16% loss in virgin flexural strength. When HGF fibers were intermingled in a carbon fiber/913 system, the loss in properties was reduced significantly but was dependent on the distance between HGFs: 8% for 70-μm HGF spacing and 2% for 200-μm HGF spacing. Although the initial flexural strength was lower for 70-μm HGF spacing, the healing performance for such HGF spacing was better than that for 200-μm HGF spacing.

3.2. Recovery of Barrier Properties

When cracks percolate or holes penetrate through the thickness of a material, barrier properties are degraded. In many applications, materials are used to prevent fluid (gas or liquid) diffusion across the material thickness and to provide a seal. Self-healing polymers and composites are capable of filling crack/hole damage to prevent transport of fluid across the material. An efficient self-sealing material is required to fill only enough damage volume to disrupt percolating cracks across the material thickness.

Current self-sealing polymers and polymer composites utilize either intrinsic or capsule-based healing approaches to seal damage induced at vastly different damage rates. Kalista and coworkers (103, 104) and Varley & van der Zwaag (105, 106) both studied the ballistic puncture and self-sealing of thin plates composed of EMAA random ionomer. Kalista and colleagues (103, 104) measured burst pressures, sometimes exceeding 3 MPa, of sealed ∼1-mm-thick EMAA. These panels were ballistically punctured at room temperature through use of a 0.51-g penetrator traveling at 196.6 m s^{-1} (9.9 J of kinetic energy). This testing protocol resulted in millimeter-size holes for unhealed ballistic puncture in LDPE. Kalista et al. proposed a two-stage healing process, shown in **Figure 9***a*, in which some of the kinetic energy of the penetrator contributes to localized friction, heating, and material extension and flow. Varley & van der Zwaag (105, 106) experimentally validated this process. In the first stage of healing, elastic recovery occurs when the molten polymer snaps back, filling the bulk of the penetrator hole. In the second stage, viscous flow occurs, resulting in interdiffusion of the molten surfaces and sealing of the remaining cracks. This EMAA ionomer can be a highly efficient intrinsic self-healing polymer in which the sealing occurs virtually at the same rate as the ballistic damage, although the healing is significantly reduced for higher ambient temperatures (103) and for loading conditions that disrupt the balance of elastic recovery and viscous flow required for sealing (105).

Recovery of barrier properties

a Ballistic puncture of ionomeric polymer

b Self-healing bladder material

c Delamination and matrix cracking in glass FRC

Recovery of corrosion protection

d Capsule-based anticorrosion

e Intrinsic anticorrosion
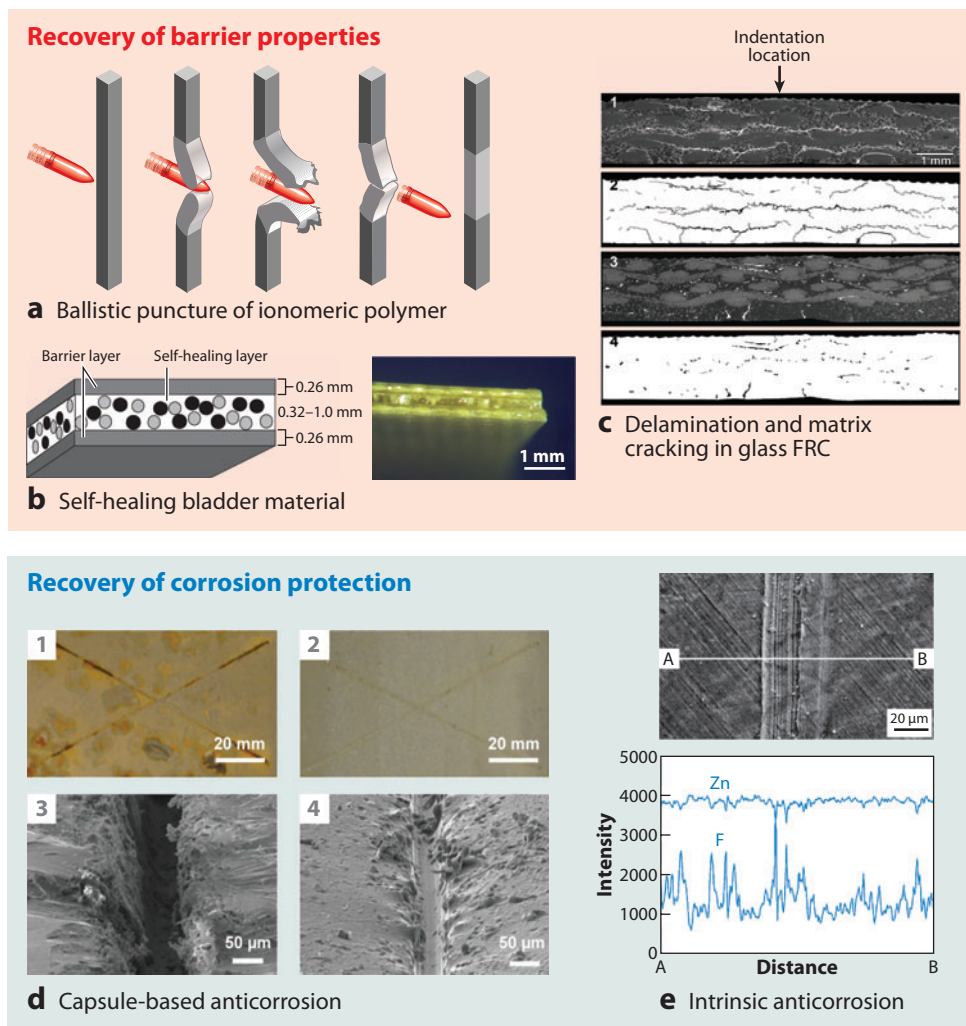
Figure 9

Self-healing for the recovery of barrier properties and corrosion resistance. (*a*) Self-healing process of ionomeric poly(ethylene-*co*-methacrylic acid) (EMAA) during ballistic puncture, for which localized heating due to friction leads to elastic recovery and viscous flow to seal the hole. Adapted from Reference 106. (*b*) Schematic (*left*) and side-view image (*right*) of a self-sealing bladder polymer composite with PDMS-tin catalyst capsule-based self-healing in the PDMS core and polyurethane-coated nylon barrier layers. Adapted from Reference 61 with permission. (*c*) Optical cross-sectional images and related highlights of cracks of an E-glass epoxy composite control specimen (images *1* and *2*) and self-sealing specimen (images *3* and *4*) after indentation and autonomic healing through use of a DCPD-Grubbs' catalyst self-healing approach. FRC denotes fiber-reinforced composite. Reprinted from Reference 41. (*d*) Optical and scanning electron micrographs of an epoxy vinyl ester coating containing a tin-catalyzed PDMS phase-separated system for control (*1*, *3*) and self-healing (*2*, *4*) systems near the surface scribe damage. Reprinted from Reference 60 with permission from Wiley-VCH. (*e*) Healed surface of a fluoro-organic coating on zinc substrate (*top*) and elemental analysis (*bottom*) showing relatively uniform fluorine concentrations over the scratched surface. Adapted from Reference 119 with permission from Wiley-VCH.

A thin PU-PDMS laminate composite from Beiermann et al. (61) and a plain-weave E-glass epoxy composite from Moll et al. (41) are two capsule-based self-sealing systems that undergo low-velocity puncture and indentation damage, respectively. The thin bladder composites of Beiermann et al. (61), with thicknesses from 0.84 mm to 1.5 mm, had a PDMS matrix central layer containing the PDMS-tin catalyst microcapsule healing system between two PU-coated ny-lon barrier layers, shown in **Figure 9b**. After puncture by insertion of hypodermic needles with diameters from 0.49 mm to 2.40 mm, the damaged laminates were allowed to heal for 24 h at room temperature, resulting in sealed pressure differentials across the thickness of up to 0.103 MPa, depending on the microcapsule size, puncture diameter, and self-healing layer thickness. Moll et al. (41) cyclically indented 4-mm-thick woven glass/epoxy composites to introduce an interpenetrating crack network through the thickness. The self-sealing specimens with a DCPD-Grubbs' catalyst healing system were allowed to heal overnight at 30°C. A 0.276-MPa pressure was applied to the specimens, and the leakage rate over 30 min was evaluated to determine sealing efficiency, which ranged from 40% to 100% depending on microcapsule size and concentration. **Figure 9c** shows a control specimen and a self-sealing specimen illustrating the reduction in crack volume for the self-sealing specimen.

3.3. Recovery of Corrosion Protection

Corrosion-resistant coatings are critical for the protection of metallic components that operate in aqueous and saline environments. The three main methods of imparting corrosion resistance are cathodic protection (124), surface passivation (125), and barrier protection. One of the limitations of barrier coatings has been the inability to prevent corrosion when the coating is scratched or abraded. To address this issue, researchers have examined the use of inorganic and sol-gel self-healing coatings. More recently, research interest has branched out to include polymeric or organic barrier coatings using both capsule-based and intrinsic systems. The standard method to assess coating self-healing behavior is through the scribing of the coating down to the substrate before environmental exposure, and the primary means of testing corrosion resistance involves the exposure of a metallic test substrate to saline solutions of known concentration through either spraying or direct immersion.

Kumar et al. (67) examined commercially synthesized urea-formaldehyde shell wall microcap-sules containing various healing agents to determine their effectiveness when incorporated into paint primer coatings for steel surfaces. Corrosion damage was assessed for scribed surfaces with ASTM D 5894 (126), a testing protocol of alternating weeklong exposure to aqueous NaCl spray and UV light. Damage was measured by optically observed undercutting of the primer coating near the scribe point. Under appropriate preparation conditions, several encapsulated compounds, including camphor and tung oil, exhibited a more-than-twofold reduction in damage as compared with microcapsule-free controls.

Suryanarayana et al. (66) examined the effectiveness of linseed oil–filled microcapsules in epoxy coatings on steel parts. Rapid film formation of the oil released from microcapsules in a coating crack plane was observed optically as the oil was activated by surface environmental exposure. Scribed samples showed no visual evidence of corrosion after exposure to salt spray for 72 h, although corrosion resistance was not quantified.

Sauvant-Moynot et al. (68) employed epoxide-based film–forming particles embedded in epoxy-amine coatings to protect steel surfaces under cathodic protection. The healing components were designed to activate only under potential within a film defect, and the barrier formation was confirmed by electrical impedance spectroscopic measurements of films before and after in situ

scribing in 0.17-M NaCl aqueous solution. The healed films exhibited temperature-dependent recovery of barrier behavior, but impedance values never reached those of undamaged films.

Cho et al. (60) examined multicomponent PDMS-based healing systems in epoxy and vinyl ester coatings on steel (**Figure 9d**). In both a phase-separated version and PU capsule-based systems, PDMS, a catalyst, and an adhesion promoter were distributed in the matrix so that the components would combine and cross-link within scratch damage. Scribed samples were allowed to heal over 24 h and then examined by optical and scanning electron microscopy and by electrical conduction measurements while immersed in 1-M NaCl aqueous solution. In the phase-separated system, a reduction in conductance of more than an order of magnitude was obtained for healed samples versus scratched controls.

A greater emphasis on surface coverage and healing of small defects over more robust mechanical properties makes intrinsic healing systems well suited for barrier protection. Several groups have investigated very different approaches to intrinsically healing films. Aramaki (115) examined the corrosion inhibition properties of a silicon-based polymer film doped with cerium(III) nitrate and water glass on zinc substrates. The release of cerium(III) nitrate into film defects effectively prevented pitting corrosion. Yabuki and coworkers examined fluoro-organic compounds as healing coatings for aluminum (118) and zinc (119). Electrical impedance measurements confirmed the recovery of corrosion resistance for samples scratched and immersed in 0.0005-M NaCl aqueous solution over 24 h. Subsequent elemental analysis showed relatively uniform fluorine concentrations over scratched surfaces, suggesting film healing (**Figure 9e**). As discussed above, Andreeva et al. tested self-healing barrier properties of PEM coatings made from PEI/PSS (116) and PEI/PSS/8HQ (117). Using scanning vibrating electrode (SVET) measurements to spatially map current density on the surface near a coating scratch, the authors showed that the PEM coating completely suppressed corrosion in 0.1-M NaCl solution over 20 h. This suppression was attributed to salt-induced breaking of ionic cross-links in the PEM film that led to the increased mobility of the constituent polyelectrolytes and coverage of the defect (117). Grigoriev et al. (69) report complete suppression of the corrosion process on an aluminum substrate via SVET measurements after immersion for 60 h in a 0.1-M NaCl solution.

4. CONCLUDING REMARKS AND FUTURE DIRECTIONS

Over the past decade, research on self-healing polymers and composites has established high performance levels for multiple material systems encompassing a wide variety of damage modes and self-healing concepts. Continued progress in the field will yield new healing chemistries that possess greater stability, higher reactivity, and faster kinetics. This nascent field of research has made great strides over the past several years, but many technical challenges remain, and there exists a great need for focused research efforts to address several areas of concern. How self-healing materials will perform under long-term environmental exposure remains an open question. Accelerated environmental testing of self-healing systems is critically needed. Although the vast majority of research on self-healing in response to fracture has focused on quasi-static performance, the ultimate utility of self-healing systems is in combating fatigue and/or periodic damage events. Relatively little research has been devoted to the dynamic aspects of self-healing under fatigue-like conditions. In addition, self-healing designs will most likely entail targeted and localized distribution of self-healing components in large-scale applications to maximize efficiency while minimizing cost and detrimental effects to the matrix material. Engineering models for design and optimization are currently lacking. Predicting the life-cycle performance of a self-healing polymer composite is currently beyond the capability of available analytical tools. Finally, for traction of the field, it is critical that a commercially successful demonstration of self-healing be achieved in

the short term. In all likelihood, this will occur for coatings first, due to a combination of their prevalence in industrial applications and their modest mechanical performance requirements. However, accelerated efforts are required to transition laboratory demonstrations into useful and practical applications across a broader cross section of industries.

Available approaches to self-healing may be applied to other material properties and performance metrics aside from the recovery of mechanical properties. Restoration of properties such as conductivity may be highly beneficial for many applications in the microelectronics industry, in which the current solution is typically chip replacement. Williams et al. (127) synthesized an organometallic polymer with semiconductor-level conductivity and the ability to self-heal with applied heat. Capsule-based or vascular approaches using conductive healing agents also show potential for restoring electrical conductivity. Balazs and coworkers (128–131) have both modeled and experimentally observed nanoparticle segregation to material defects, which may be applied to conductive particles in conductive substrates.

Restoration of optical properties may also be a favorable path for self-healing research. Cracking in materials disrupts transparency due to light scattering, and the application of an index-matched polymer is often used to mitigate that effect. The ability to deliver an index-matched fluid through a vascular or a capsule-based system may enable autonomous recovery of transparency. Intrinsic self-healing of optically relevant materials may also eliminate scattering by healing any generated cracks.

The full range of opto-electronic, mechanical, and chemical properties of materials, from dielectric behavior to optical transmission to chemical stability, may be addressed using self-healing concepts. Wherever materials are used, self-healing concepts may lead to enhanced utility. Longer life, safer self-healing batteries, resealing tires, fade-resistant fabrics, and antitamper electronics are all potential applications for self-healing concepts. Yet what lies beyond healing? Biological systems again provide a road map for potential research paths. Many critically important biological materials, for example, bone, regenerate and remodel. In the future, synthetic materials that currently heal in response to damage may one day respond in a more regulated fashion so that regeneration and remodeling occur over the lifetime of the material in response to mechanical loading.

SUMMARY POINTS

1. Self-healing polymers have been demonstrated utilizing three main concepts: (*a*) capsule-based healing, (*b*) vascular healing, and (*c*) intrinsic healing.

2. Capsule-based approaches are easily integrated in most polymer systems, but their function is locally depleted after a single damage event.

3. Vascular approaches hold great promise for healing large damage volumes over multiple damage events, but their integration in existing material systems is challenging.

4. Intrinsic healing approaches are elegant but limited to small damage volumes because intimate material contact is required for healing.

5. A wide variety of self-healing polymers—thermosets, thermoplastics, and elastomers— have been demonstrated to date. Self-healing fiber-reinforced composites have been demonstrated to a lesser degree, and they pose many technical challenges to integration.

6. For all self-healing systems, material stasis is achieved when the rate of healing is equal to the rate of damage.

DISCLOSURE STATEMENT

ACKNOWLEDGMENTS

LITERATURE CITED

1. van der Zwaag S. 2007. *Self Healing Materials: An Alternative Approach to 20 Centuries of Materials Science*. Dordrecht: Springer-Verlag
2. Bergman SD, Wudl F. 2008. Mendable polymers. *J. Mater. Chem.* 18(1):41–62
3. Wool RP. 2008. Self-healing materials: a review. *Soft Matter* 4(3):400–18
4. Wu DY, Meure S, Solomon D. 2008. Self-healing polymeric materials: a review of recent developments. *Prog. Polym. Sci.* 33(5):479–522
5. Kessler MR. 2007. Self-healing: a new paradigm in materials design. *Proc. Inst. Mech. Eng. G* 221(4):479–95
6. Yuan YC, Yin T, Rong MZ, Zhang MQ. 2008. Self healing in polymers and polymer composites. Concepts, realization and outlook: a review. *Express Polym. Lett.* 2(4):238–50
7. Youngblood JP, Sottos NR, Extrand C. 2008. Bioinspired materials for self-cleaning and self-healing. *MRS Bull.* 33(8):732–41
8. Williams KA, Dreyer DR, Bielawski CW. 2008. The underlying chemistry of self-healing materials. *MRS Bull.* 33(8):759–65
9. White SR, Caruso MM, Moore JS. 2008. Autonomic healing of polymers. *MRS Bull.* 33(8):766–69
10. Bond IP, Trask RS, Williams HR. 2008. Self-healing fiber-reinforced polymer composites. *MRS Bull.* 33:770–74
11. Trask RS, Williams HR, Bond IP. 2007. Self-healing polymer composites: mimicking nature to enhance performance. *Bioinspiration Biomim.* 2(1):1–9
12. Kondō A, Van Valkenburg JW. 1979. *Microcapsule Processing and Technology*. New York: Marcel Dekker
13. Benita S, ed. 2006. *Microencapsulation: Methods and Industrial Applications*. Boca Raton, FL: CRC/Taylor & Francis
14. Ghosh SK, ed. 2006. *Functional Coatings: By Polymer Microencapsulation*. Weinheim: Wiley-VCH
15. Brown EN, Kessler MR, Sottos NR, White SR. 2003. In situ poly(urea-formaldehyde) microencapsulation of dicyclopentadiene. *J. Microencapsul.* 20(6):719–30
16. Blaiszik BJ, Sottos NR, White SR. 2008. Nanocapsules for self-healing materials. *Compos. Sci. Technol.* 68(3–4):978–86
17. Blaiszik BJ, Caruso MM, McIlroy DA, Moore JS, White SR, Sottos NR. 2009. Microcapsules filled with reactive solutions for self-healing materials. *Polymer* 50(4):990–97
18. Keller MW, White SR, Sottos NR. 2007. A self-healing poly(dimethyl siloxane) elastomer. *Adv. Funct. Mater.* 17(14):2399–404
19. Yuan L, Liang GZ, Xie JQ, Li L, Guo J. 2006. Preparation and characterization of poly(urea-formaldehyde) microcapsules filled with epoxy resins. *Polymer* 47(15):5338–49
20. Cosco S, Ambrogi V, Musto P, Carfagna C. 2007. Properties of poly(urea-formaldheyde) microcapsules containing an epoxy resin. *J. Appl. Polym. Sci.* 105(3):1400–11

21. Yuan YC, Rong MZ, Zhang MQ, Chen B, Yang GC, Li XM. 2008. Self-healing polymeric materials using epoxy/mercaptan as the healant. *Macromolecules* 41(14):5197–202

22. Yuan YC, Rong MZ, Zhang MQ. 2008. Preparation and characterization of microencapsulated polythiol. *Polymer* 49(10):2531–41

23. Yuan YC, Rong MZ, Zhang MQ. 2008. Preparation and characterization of poly (melamine-formaldehyde) walled microcapsules containing epoxy. *Acta Polym. Sin.* (5):472–80

24. Liu X, Sheng X, Lee JK, Kessler MR. 2009. Synthesis and characterization of melamine-urea-formaldehyde microcapsules containing ENB-based self-healing agents. *Macromol. Mater. Eng.* 294(6–7):389–95

25. Cho SH, Andersson HM, White SR, Sottos NR, Braun PV. 2006. Polydimethylsiloxane-based self-healing materials. *Adv. Mater.* 18(8):997–1000

26. Xiao DS, Yuan YC, Rong MZ, Zhang MQ. 2009. Hollow polymeric microcapsules: preparation, characterization and application in holding boron trifluoride diethyl etherate. *Polymer* 50(2):560–68

27. Rule JD, Brown EN, Sottos NR, White SR, Moore JS. 2005. Wax-protected catalyst microspheres for efficient self-healing materials. *Adv. Mater.* 17(2):205–8

28. Yeom CK, Oh SB, Rhim JW, Lee JM. 2000. Microencapsulation of water-soluble herbicide by interfacial reaction. I. Characterization of microencapsulation. *J. Appl. Polym. Sci.* 78(9):1645–55

29. Mookhoek SD, Blaiszik BJ, Fischer HR, Sottos NR, White SR, van der Zwaag S. 2008. Peripherally decorated binary microcapsules containing two liquids. *J. Mater. Chem.* 18(44):5390–94

30. Voorn DJ, Ming W, van Herk AM. 2006. Polymer-clay nanocomposite latex particles by inverse pickering emulsion polymerization stabilized with hydrophobic montmorillonite platelets. *Macromolecules* 39(6):2137–43

31. Abate AR, Weitz DA. 2009. High-order multiple emulsions formed in poly(dimethylsiloxane) microfluidics. *Small* 5(18):2030–32

32. White SR, Sottos NR, Geubelle PH, Moore JS, Kessler MR, et al. 2001. Autonomic healing of polymer composites. *Nature* 409(6822):794–97

33. Brown EN, Sottos NR, White SR. 2002. Fracture testing of a self-healing polymer composite. *Exp. Mech.* 42(4):372–79

34. Brown EN, White SR, Sottos NR. 2005. Retardation and repair of fatigue cracks in a microcapsule toughened epoxy composite. 1. Manual infiltration. *Compos. Sci. Technol.* 65(15–16):2466–73

35. Brown EN, White SR, Sottos NR. 2005. Retardation and repair of fatigue cracks in a microcapsule toughened epoxy composite. II. In situ self-healing. *Compos. Sci. Technol.* 65(15–16):2474–80

36. Brown EN, White SR, Sottos NR. 2004. Microcapsule induced toughening in a self-healing polymer composite. *J. Mater. Sci.* 39(5):1703–10

37. Rule JD, Sottos NR, White SR. 2007. Effect of microcapsule size on the performance of self-healing polymers. *Polymer* 48(12):3520–29

38. Kirkby EL, Rule JD, Michaud VL, Sottos NR, White SR, Manson JAE. 2008. Embedded shape-memory alloy wires for improved performance of self-healing polymers. *Adv. Funct. Mater.* 18(15):2253–60

39. Jones AS, Rule JD, Moore JS, Sottos NR, White SR. 2007. Life extension of self-healing polymers with rapidly growing fatigue cracks. *J. R. Soc. Interface* 4(13):395–403

40. Kirkby EL, Michaud VJ, Manson JAE, Sottos NR, White SR. 2009. Performance of self-healing epoxy with microencapsulated healing agent and shape memory alloy wires. *Polymer* 50(23):5533–38

41. Moll JL, White SR, Sottos NR. 2010. A self-sealing fiber reinforced composite. *J. Compos. Mater.* In press; doi: 10.1177/0021998309356605

42. Kessler MR, Sottos NR, White SR. 2003. Self-healing structural composite materials. *Composites A* 34(8):743–53

43. Patel AJ, Sottos NR, Wetzel ED, White SR. 2010. Autonomic healing of low-velocity impact damage in fiber-reinforced composites. *Composites A* 41(3):360–68

44. Kessler MR, White SR. 2001. Self-activated healing of delamination damage in woven composites. *Composites A* 32(5):683–99

45. Sanada K, Yasuda I, Shindo Y. 2006. Transverse tensile strength of unidirectional fiber-reinforced polymers and self-healing of interfacial debonding. *Plast. Rubber Compos.* 35(2):67–72

46. Wilson GO, Moore JS, White SR, Sottos NR, Andersson HM. 2008. Autonomic healing of epoxy vinyl esters via ring opening metathesis polymerization. *Adv. Funct. Mater.* 18(1):44–52

47. Chipara MD, Chipara M, Shansky E, Zaleski JM. 2009. Self-healing of high elasticity block copolymers. *Polym. Adv. Technol.* 20(4):427–31

48. Maiti S, Geubelle PH. 2006. Cohesive modeling of fatigue crack retardation in polymers: crack closure effect. *Eng. Fract. Mech.* 73(1):22–41

49. Maiti S, Shankar C, Geubelle PH, Kieffer J. 2006. Continuum and molecular-level modeling of fatigue crack retardation in self-healing polymers. *J. Eng. Mater. Technol. Trans. ASME* 128(4):595–602

50. Wilson GO, Caruso MM, Reimer NT, White SR, Sottos NR, Moore JS. 2008. Evaluation of ruthenium catalysts for ring-opening metathesis polymerization-based self-healing applications. *Chem. Mater.* 20(10):3288–97

51. Wilson GO, Porter KA, Weissman H, White SR, Sottos NR, Moore JS. 2009. Stability of second generation Grubbs' alkylidenes to primary amines: formation of novel ruthenium-amine complexes. *Adv. Synth. Catal.* 351(11–12):1817–25

52. Liu X, Lee JK, Yoon SH, Kessler MR. 2006. Characterization of diene monomers as healing agents for autonomic damage repair. *J. Appl. Polym. Sci.* 101(3):1266–72

53. Kamphaus JM, Rule JD, Moore JS, Sottos NR, White SR. 2008. A new self-healing epoxy with tungsten (VI) chloride catalyst. *J. R. Soc. Interface* 5(18):95–103

54. Rong MZ, Zhang MQ, Zhang W. 2007. A novel self-healing epoxy system with microencapsulated epoxy and imidazole curing agent. *Adv. Compos. Lett.* 16(5):167–72

55. Yin T, Zhou L, Rong MZ, Zhang MQ. 2008. Self-healing woven glass fabric/epoxy composites with the healant consisting of microencapsulated epoxy and latent curing agent. *Smart Mater. Struct.* 17(1):015019/1–8

56. Yin T, Rong MZ, Zhang MQ, Zhao JQ. 2009. Durability of self-healing woven glass fabric/epoxy composites. *Smart Mater. Struct.* 18(7):074001

57. Yin T, Rong MZ, Wu JS, Chen HB, Zhang MQ. 2008. Healing of impact damage in woven glass fabric reinforced epoxy composites. *Composites A* 39(9):1479–87

58. Yin T, Rong MZ, Zhang MQ, Yang GC. 2007. Self-healing epoxy composites: preparation and effect of the healant consisting of microencapsulated epoxy and latent curing agent. *Compos. Sci. Technol.* 67(2):201–12

59. Keller MW, White SR, Sottos NR. 2008. Torsion fatigue response of self-healing poly (dimethylsiloxane) elastomers. *Polymer* 49(13–14):3136–45

60. Cho SH, White SR, Braun PV. 2009. Self-healing polymer coatings. *Adv. Mater.* 21(6):645–49

61. Beiermann BA, Keller MW, Sottos NR. 2009. Self-healing flexible laminates for resealing of puncture damage. *Smart Mater. Struct.* 18(8):085001

62. Xiao DS, Yuan YC, Rong MZ, Zhang MQ. 2009. Self-healing epoxy based on cationic chain polymerization. *Polymer* 50(13):2967–75

63. Caruso MM, Delafuente DA, Ho V, Sottos NR, Moore JS, White SR. 2007. Solvent-promoted self-healing epoxy materials. *Macromolecules* 40(25):8830–32

64. Caruso MM, Blaiszik BJ, White SR, Sottos NR, Moore JS. 2008. Full recovery of fracture toughness using a nontoxic solvent-based self-healing system. *Adv. Funct. Mater.* 18(13):1898–904

65. Zako M, Takano N. 1999. Intelligent material systems using epoxy particles to repair microcracks and delamination damage in GFRP. *J. Intell. Mater. Syst. Struct.* 10(10):836–41

66. Suryanarayana C, Rao KC, Kumar D. 2008. Preparation and characterization of microcapsules containing linseed oil and its use in self-healing coatings. *Prog. Org. Coat.* 63(1):72–78

67. Kumar A, Stephenson L, Murray J. 2006. Self-healing coatings for steel. *Prog. Org. Coat.* 55(3):244–53

68. Sauvant-Moynot V, Gonzalez S, Kittel J. 2008. Self-healing coatings: an alternative route for anticorrosion protection. *Prog. Org. Coat.* 63(3):307–15

69. Grigoriev DO, Kohler K, Skorb E, Shchukin DG, Mohwald H. 2009. Polyelectrolyte complexes as a "smart" depot for self-healing anticorrosion coatings. *Soft Matter* 5(7):1426–32

70. Huang J, Kim J, Agrawal N, Sudarsan AP, Maxim JE, et al. 2009. Rapid fabrication of bio-inspired 3D microfluidic vascular networks. *Adv. Mater.* 21(35):3567–71

71. Dry CM, Sottos NR. 1993. Passive smart self-repair in polymer matrix composite materials. In *Smart Structures and Materials 1993: Smart Materials, SPIE Proc., Feb. 1–4*, 1916:438–44. Albuquerque, NM: Soc. Photo-Opt. Instrum. Eng.

72. Dry CM. 1996. Procedures developed for self-repair of polymer matrix composite materials. *Compos. Struct.* 35(3):263–69

73. Motuku M, Vaidya UK, Janowski GM. 1999. Parametric studies on self-repairing approaches for resin infused composites subjected to low velocity impact. *Smart Mater. Struct.* 8(5):623–38

74. Bleay SM, Loader CB, Hawyes VJ, Humberstone L, Curtis PT. 2001. A smart repair system for polymer matrix composites. *Composites A* 32(12):1767–76

75. Pang JWC, Bond IP. 2005. 'Bleeding composites': damage detection and self-repair using a biomimetic approach. *Composites A* 36(2):183–88

76. Pang JWC, Bond IP. 2005. A hollow fiber reinforced polymer composite encompassing self-healing and enhanced damage visibility. *Compos. Sci. Technol.* 65(11–12):1791–99

77. Trask R, Bond I. 2006. Biomimetic self-healing of advanced composite structures using hollow glass fibres. *Smart Mater. Struct.* 15(3):704–10

78. Williams GJ, Trask RS, Bond IP. 2007. A self-healing carbon fiber reinforced polymer for aerospace applications. *Composites A* 38(6):1525–32

79. Trask RS, Williams GJ, Bond IP. 2007. Bioinspired self-healing of advanced composite structures using hollow glass fibres. *J. R. Soc. Interface* 4(13):363–71

80. Williams HR, Trask RS, Weaver PM, Bond IP. 2008. Minimum mass vascular networks in multifunctional materials. *J. R. Soc. Interface* 5(18):55–65

81. Williams HR, Trask RS, Knights AC, Williams ER, Bond IP. 2008. Biomimetic reliability strategies for self-healing vascular networks in engineering materials. *J. R. Soc. Interface* 5(24):735–47

82. Kim S, Lorente S, Bejan A. 2006. Vascularized materials: tree-shaped flow architectures matched canopy to canopy. *J. Appl. Phys.* 100(6):63525

83. Zhang HL, Lorente S, Bejan A. 2007. Vascularization with trees that alternate with upside-down trees. *J. Appl. Phys.* 101(9):094904

84. Lorente S, Bejan A. 2009. Vascularized smart materials: designed porous media for self-healing and self-cooling. *J. Porous Media* 12(1):1–18

85. Wang KM, Lorente S, Bejan A. 2006. Vascularized networks with two optimized channel sizes. *J. Phys. D* 39(14):3086–96

86. Williams HR, Trask RS, Bond IP. 2007. Self-healing composite sandwich structures. *Smart Mater. Struct.* 16(4):1198–207

87. Williams HR, Trask RS, Bond IP. 2008. Self-healing sandwich panels: restoration of compressive strength after impact. *Compos. Sci. Technol.* 68(15–16):3171–77

88. Aragón AM, Wayer JK, Geubelle PH, Goldberg DE, White SR. 2008. Design of microvascular flow networks using multi-objective genetic algorithms. *Comput. Methods Appl. Mech. Eng.* 197(49–50):4399–410

89. Toohey KS, Sottos NR, Lewis JA, Moore JS, White SR. 2007. Self-healing materials with microvascular networks. *Nat. Mater.* 6(8):581–85

90. Toohey KS, Sottos NR, White SR. 2009. Characterization of microvascular-based self-healing coatings. *Exp. Mech.* 49(5):707–17

91. Toohey KS, Hansen CJ, Lewis JA, White SR, Sottos NR. 2009. Delivery of two-part self-healing chemistry via microvascular networks. *Adv. Funct. Mater.* 19(9):1399–405

92. Hansen CJ, Wu W, Toohey KS, Sottos NR, White SR, Lewis JA. 2009. Self-healing materials with interpenetrating microvascular networks. *Adv. Mater.* 21(41):4143–47

93. Chen XX, Dam MA, Ono K, Mal A, Shen HB, et al. 2002. A thermally remendable cross-linked polymeric material. *Science* 295(5560):1698–702

94. Chen XX, Wudl F, Mal AK, Shen HB, Nutt SR. 2003. New thermally remendable highly cross-linked polymeric materials. *Macromolecules* 36(6):1802–7

95. Plaisted TA, Nemat-Nasser S. 2007. Quantitative evaluation of fracture, healing and rehealing of a reversibly cross-linked polymer. *Acta Mater.* 55(17):5684–96

96. Park JS, Takahashi K, Guo ZH, Wang Y, Bolanos E, et al. 2008. Towards development of a self-healing composite using a mendable polymer and resistive heating. *J. Compos. Mater.* 42(26):2869–81

97. Park JS, Kim HS, Hahn HT. 2009. Healing behavior of a matrix crack on a carbon fiber/mendomer composite. *Compos. Sci. Technol.* 69(7–8):1082–87

98. Murphy EB, Bolanos E, Schaffner-Hamann C, Wudl F, Nutt SR, Auad ML. 2008. Synthesis and characterization of a single-component thermally remendable polymer network: Staudinger and Stille revisited. *Macromolecules* 41(14):5203–9

99. Peterson AM, Jensen RE, Palmese GR. 2009. Reversibly cross-linked polymer gels as healing agents for epoxy-amine thermosets. *Appl. Mater. Interfaces* 1(5):992–95

100. Hayes SA, Zhang W, Branthwaite M, Jones FR. 2007. Self-healing of damage in fiber-reinforced polymer-matrix composites. *J. R. Soc. Interface* 4(13):381–87

101. Hayes SA, Jones FR, Marshiya K, Zhang W. 2007. A self-healing thermosetting composite material. *Composites A* 38(4):1116–20

102. Luo XF, Ou RQ, Eberly DE, Singhal A, Viratyaporn W, Mather PT. 2009. A thermoplastic/thermoset blend exhibiting thermal mending and reversible adhesion. *ACS Appl. Mater. Interfaces* 1(3):612–20

103. Kalista SJ, Ward TC, Oyetunji Z. 2007. Self-healing of poly(ethylene-comethacrylic acid) copolymers following projectile puncture. *Mech. Adv. Mater. Struct.* 14(5):391–97

104. Kalista S, Ward T. 2007. Thermal characteristics of the self-healing response in poly(ethylene-comethacrylic acid) copolymers. *J. R. Soc. Interface* 4(13):405–11

105. Varley RJ, van der Zwaag S. 2008. Towards an understanding of thermally activated self-healing of an ionomer system during ballistic penetration. *Acta Mater.* 56(19):5737–50

106. Varley RJ, van der Zwaag S. 2008. Development of a quasi-static test method to investigate the origin of self-healing in ionomers under ballistic conditions. *Polym. Test.* 27(1):11–19

107. Cordier P, Tournilhac F, Soulie-Ziakovic C, Leibler L. 2008. Self-healing and thermoreversible rubber from supramolecular assembly. *Nature* 451(7181):977–80

108. Montarnal D, Tournilhac F, Hidalgo M, Couturier J, Leibler L. 2009. Versatile one-pot synthesis of supramolecular plastics and self-healing rubbers. *J. Am. Chem. Soc.* 131(23):7966–67

109. O'Connor K, Wool R. 1980. Optical studies of void formation and healing in styrene-isoprene-styrene block copolymers. *J. Appl. Phys.* 51(10):5075–79

110. Wool R, O'Connor K. 1981. Theory of crack healing in polymers. *J. Appl. Phys.* 52(10):5953–63

111. McGarel JO, Wool RP. 1987. Craze growth and healing in polystyrene. *J. Polym. Sci. B* 25(12):2541–60

112. Yamaguchi M, Ono S, Okamoto K. 2009. Interdiffusion of dangling chains in weak gel and its application to self-repairing material. *Mater. Sci. Eng. B* 162(3):189–94

113. Yamaguchi M, Ono S, Terano M. 2007. Self-repairing property of polymer network with dangling chains. *Mater. Lett.* 61(6):1396–99

114. Rahmathullah MAM, Palmese GR. 2009. Crack-healing behavior of epoxy-amine thermosets. *J. Appl. Polym. Sci.* 113(4):2191–201

115. Aramaki K. 2002. Preparation of chromate-free, self-healing polymer films containing sodium silicate on zinc pretreated in a cerium(III) nitrate solution for preventing zinc corrosion at scratches in 0.5 M NaCl. *Corros. Sci.* 44(6):1375–89

116. Andreeva DV, Fix D, Mohwald H, Shchukin DG. 2008. Buffering polyelectrolyte multilayers for active corrosion protection. *J. Mater. Chem.* 18(15):1738–40

117. Andreeva DV, Fix D, Mohwald H, Shchukin DG. 2008. Self-healing anticorrosion coatings based on pH-sensitive polyelectrolyte/inhibitor sandwichlike nanostructures. *Adv. Mater.* 20(14):2789–94

118. Yabuki A, Yamagami H, Noishiki K. 2007. Barrier and self-healing abilities of corrosion protective polymer coatings and metal powders for aluminum alloys. *Mater. Corros.* 58(7):497–501

119. Yabuki A, Kaneda R. 2009. Barrier and self-healing coating with fluoro-organic compound for zinc. *Mater. Corros.* 60(6):444–49

120. Brown EN, White SR, Sottos NR. 2006. Fatigue crack propagation in microcapsule-toughened epoxy. *J. Mater. Sci.* 41(19):6266–73

121. Mostovoy S, Crosley PB, Ripling EJ. 1967. Use of crack-line-loaded specimens for measuring plane-strain fracture toughness. *J. Mater.* 2(3):661–81

122. Kessler MR, White SR. 2002. Cure kinetics of the ring-opening metathesis polymerization of dicy-clopentadiene. *J. Polym. Sci. A* 40(14):2373–83

123. Williams GJ, Bond IP, Trask RS. 2009. Compression after impact assessment of self-healing CFRP. *Composites A* 40(9):1399–406

124. Pérez N. 2004. Cathodic protection. In *Electrochemistry and Corrosion Science*, ed. N Pérez, pp. 247–94. Boston: Kluwer Acad.

125. Maurice V, Marcus P. 2009. Structure, passivation and localized corrosion of metal surfaces. In *Progress in Corrosion Science and Engineering I*, ed. SI Pyun, JW Lee, pp. 1–58. New York: Springer

126. Baboian R, ed. 2005. *Corrosion Tests and Standards: Application and Interpretation*. West Conshohocken, PA: ASTM Int. 2nd ed.

127. Williams KA, Boydston AJ, Bielawski CW. 2007. Towards electrically conductive, self-healing materials. *J. R. Soc. Interface* 4(13):359–62

128. Lee JY, Buxton GA, Balazs AC. 2004. Using nanoparticles to create self-healing composites. *J. Chem. Phys.* 121(11):5531–40

129. Balazs AC, Emrick T, Russell TP. 2006. Nanoparticle polymer composites: where two small worlds meet. *Science* 314(5802):1107–10

130. Gupta S, Qingling Z, Emrick T, Balazs A, Russell T. 2006. Entropy-driven segregation of nanoparticles to cracks in multilayered composite polymer structures. *Nat. Mater.* 5(3):229–33

131. Balazs AC. 2007. Modeling self-healing materials. *Mater. Today* 10(9):18–23

Contents

Index

Errata

An online log of corrections to *Annual Review of Materials Research* articles may be
found at http://matsci.annualreviews.org/errata.shtml